

Article

Towards a Biorefinery Processing Waste from Plantain Agro-Industry: Process Design and Techno-Economic Assessment of Single-Cell Protein, Natural Fibers, and Biomethane Production through Process Simulation

James A. Gómez ^{1,2}, Luis G. Matallana ³ and Óscar J. Sánchez ^{3,*}

¹ Research Group on Food and Agro-Industry, Faculty of Engineering, Universidad de Caldas, Calle 65 No. 26 10, Manizales 170004, Colombia

² CEB—Centre of Biological Engineering, University of Minho, Campus de Gualtar, 4710-057 Braga, Portugal

³ CTD—Bioprocess and Agro-Industry Plant, Department of Engineering, Universidad de Caldas, Calle 65 No. 26-10, Manizales 170004, Colombia

* Correspondence: osanchez@ucaldas.edu.co; Tel.: +57-6-8781500

Citation: Gómez, J.A.; Matallana, L.G.; Sánchez, Ó.J. Towards a Biorefinery Processing Waste from Plantain Agro-Industry: Process Design and Techno-Economic Assessment of Single-Cell Protein, Natural Fibers, and Biomethane Production through Process Simulation. *Fermentation* **2022**, *8*, 582. <https://doi.org/10.3390/fermentation8110582>

Academic Editors: Aijuan Zhou, Cristiano Varrone and Zhangwei He

Received: 4 October 2022

Accepted: 21 October 2022

Published: 27 October 2022

Publisher's Note: MDPI stays neutral with regard to jurisdictional claims in published maps and institutional affiliations.



Copyright: © 2022 by the authors. Licensee MDPI, Basel, Switzerland. This article is an open access article distributed under the terms and conditions of the Creative Commons Attribution (CC BY) license (<https://creativecommons.org/licenses/by/4.0/>).

Abstract: The plantain agro-industry generates different residues in the harvest and post-harvest stages. Therefore, the design of processes for valorization is required. The aim of this work was to design and techno-economically evaluate the processes for the production of single-cell protein, natural fibers, and biomethane from plantain residues by process simulation in the framework of the design of a future biorefinery for valorization of these residues. The processes were simulated using SuperPro Designer. The scale size was calculated at 1,267,071 tons for the processing of plantain lignocellulosic waste (pseudostems) and 3179 tons for the processing of starchy waste (rejected unripe plantain fruits). The results obtained suggest that the best alternative for the valorization of plantain residues corresponded to the production of natural fibers, with a net present value of \$29,299,000. This work shows that waste from the plantain agro-industry exhibits high potential as a feedstock for the production of value-added products. In addition, the process flowsheets simulated in this work can be integrated into the basic design of a biorefinery processing plantain waste.

Keywords: anaerobic digestion; cellulose hydrolysis; *Musa AAB Simmonds*; process flowsheeting; process scheduling; starch hydrolysis

1. Introduction

The global production of residues is increasing; therefore, it is necessary to design new processes or improve existing ones for valorization [1]. The global production of agricultural waste estimated from data reported by FAO [2] was 386,135 million tons in 2019. In Colombia, the generation of agricultural waste from the most representative crops (rice, beans, and corn, among others) was calculated at about 540 million tons [2]. The wastes of plantain cropping were calculated at about 25 million tons [2,3].

During the cropping, harvesting, and post-harvesting of plantain, only 20% to 30% of the plant is used [4]. The remaining biomass, such as pseudostems, rachis, and rejected unripe plantain fruits (RUPFs, fruits that do not meet the quality standards in the harvest and post-harvest stages), is left on the parcels or is disposed of as municipal solid waste [5,6]. In Colombia, a middle-income member country of the OECD, the Dominico-Hartón plantain (*Musa AAB Simmonds*) is one of the most cultivated varieties for human consumption [7].

The main components of plantain waste are cellulose, hemicellulose, and starch [8]. These compounds can be recovered through physical, thermochemical, chemical, and biological processes in the context of a biorefinery to obtain fermentable sugars and other products [5]. Biorefineries are sustainable production systems that recover a considerable amount of carbon from the biomass in a broad and innovative portfolio of marketable products, such as food, feed, biofuel, and energy, among others [9]. In this regard, the production of single-cell protein (SCP), natural fibers (NFs), and biomethane (BM) represents options for valorization of the waste from the plantain agro-industry in a profitable way.

SCP refers to dried microbial cells from bacteria, yeast, fungi, or algae, which serves as feed or food supplements grown in large-scale fermentation systems for use as protein sources in human food or animal feed [10]. On the other hand, NFs can be classified into animal, plant, and mineral fibers. Fibers obtained from animal hairs or secreted by animals are known as animal fibers (protein-based); wool and silk fibers are the main examples of animal fibers. Plant fibers are obtained from different plants and their main component is cellulose; flax, hemp, jute, ramie, and kenaf are examples of plant fibers. Mineral fibers are inorganic fibers that are produced naturally, such as asbestos, fibrous brucite, and wollastonite [11,12]. Biogas is a product of anaerobic digestion, where microorganisms break down organic materials in the absence of oxygen. Biogas mainly consists of methane, carbon dioxide, and low amounts of water vapor, hydrogen sulfide, and other trace gases [13]. When CO₂, H₂O, H₂S, and other gases are removed from biogas, it is considered biomethane. All these processes require feedstocks with a high content of fermentable sugars (or polysaccharides that can be hydrolyzed into sugars) or polymers organized into fibers. Plantain residue can provide this type of compound, considering its high contents of lignocellulosic materials.

Different studies have been conducted that aimed to valorize plantain residues. Plantain fruits, peels [14,15], banana peels, and ripe bananas have been used to obtain SCP [16,17]. The production and use of NFs from the pseudostems and rachis of plantain plants to reinforce materials have been studied [18,19], and BM production from plantain peels has been reported [20–22]. Likewise, whole unripe plantain fruits and pseudostems from *Musa paradisiaca* L. were proposed as feedstocks for bioethanol production [23]. Different works have reported the use of Musaceae waste and other residues to produce silage [24–26] and nutrient blocks [27–31] for animal feed. Nevertheless, to our knowledge, the design and techno-economic analysis of independent processes for producing SCP, NFs, and BM from Dominico-Hartón plantain waste using process simulation techniques have never been studied.

The use of computer-aided process design tools can allow the exploration of multiple alternatives for the conversion of plantain waste into SCP, NFs, and BM. Likewise, the determination of the best viable option for each one of these processes via simulation has the potential to support future research efforts to improve and develop this type of valorization technology.

Simulation-based techno-economic assessment supports decision-makers in their selection of the most appropriate valorization technology that could be implemented on small or large scales in regions with a high availability of plantain waste. Techno-economic assessment is an activity for setting large-scale processes, mainly on an industrial scale. Techno-economic assessment combines process modeling and engineering design with economic evaluation, and helps to assess the economic viability of both process flow-sheet configurations and biobased products [32]. In addition, these valorization processes can be analyzed as alternative processing pathways within a biorefinery using plantain waste as the feedstock. This may contribute to a reduction in the environmental impact caused by agricultural activities and support the transition from a linear to a circular economy to achieve a more sustainable society [33]. Therefore, the aim of this work was to design and techno-economically assess several processes for the production of SCP, NFs,

and BM from the waste of the plantain agro-industry through process simulation in order to determine their viability for a large scale.

2. Methodological Approach

2.1. Process Development

2.1.1. Scale Definition

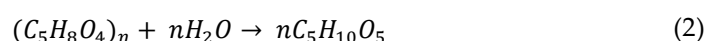
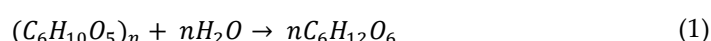
The definition of the scale for the simulation of the processes proposed was calculated from the information obtained from primary and secondary sources (plantain plantation and databases) and by applying different forecasting methods as discussed in previous works [8,34].

2.1.2. Data Collection

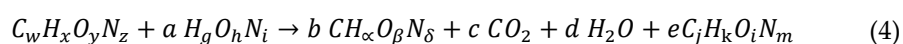
Data collection for the design of valorization processes was carried out according to the procedure described in previous works [8,34]. The data collection focused on identifying operating conditions and technological configurations for the production of SCP, NFs, and BM using different feedstock streams (lignocellulosic and starchy materials from plantain waste).

2.1.3. Process Design and Simulation

The design of the processes was carried out in two stages: conceptual design and basic design, as discussed in previous works [8,34]. The conceptual design was built from the data collected in the databases and using the ISO 10628-1, *Diagrams for the chemical and petrochemical industry* [35]. MS Visio (Microsoft Corporation, USA) was used to represent unit operations and unit processes through the engineering symbols. Then, each process was described. The basic design of the processes proposed (represented by the process flowsheets) was performed using the SuperPro Designer v10 simulator (Intelligen, Inc., USA) and following the simulation procedure described in previous works [8,34]. The chemical reactions reported by Wyman et al. [36] for the hydrolysis of starch and cellulose $(C_6H_{10}O_5)_n$ into glucose $(C_6H_{12}O_6)$, and hemicellulose $(C_5H_8O_4)_n$ into xylose $(C_5H_{10}O_5)$ were used to deduce the reaction system of the designed processes. These reactions were entered into the reactor modules of the simulator (the modules representing a unit operation or unit process are called unit procedures in the SuperPro Designer interface) as follows:



The equations described by Doran [37] for aerobic and anaerobic cell growth were entered into the fermenter modules and used to represent microbial cultivation processes:



where $C_wH_xO_yN_z$ is the chemical formula for the carbon source or substrate; $H_gO_hN_i$ is the chemical formula for the nitrogen source (e.g., for ammonia NH_3 , $g=3$, $h=0$, and $i=1$); $CH_\alpha O_\beta N_\delta$ is the chemical formula for dry cells; and $C_jH_kO_lN_m$ considers the formation of an extracellular product.

The *C. utilis* formula ($CH_{1.84}O_{0.56}N_{0.2}$) was used in the reaction (3) for the SCP production [38], and was entered into the fermenter modules of the simulator. The stoichiometry described by Angelidaki et al. [39,40] was employed to define the reactions of BM production, which were entered into the digester modules of the simulator. The molecular formulas of bacterial biomass ($C_5H_7NO_2$), glycerol trioleate ($C_{57}H_{104}O_6$), long-chain fatty acids (LCFAs, $C_{18}H_{34}O_2$) as a standard lipid, and proteins ($CH_{2.03}O_{0.60}N_{0.3}S_{0.001}$) were used in the reactions for cell growth [41].

The Monod model was employed to represent the cell growth kinetics for fermenters and digesters, as described by Diwekar [42]; for product formation, the following expression was considered:

$$\frac{dP}{dt} = \mu_{max} Y_{P/S} \frac{SX}{K_s + S}$$

where P is the product concentration (g/L), μ_{max} is the maximal specific growth rate (h^{-1}), $Y_{P/S}$ is the product yield coefficient from the substrate (g/g), S is the substrate concentration (g/L), K_s is the half-saturation constant (g/L), and X is the cell concentration (g/L). The kinetic constants $\mu_{max} = 0.38 \text{ h}^{-1}$ and $K_s = 2.59 \text{ g/L}$ were used in the growth equations for *C. utilis* growth [38], which were entered into the fermenter modules of the simulator. The kinetic constants used in the equations describing biomass growth and biomethane production during anaerobic digestion are shown in Table 1. All reactions were algebraically balanced by applying an optimization routine using the `fmincon` MATLAB function; then, the simulation procedure described in previous works was followed [8,34].

Table 1. Kinetic constants of the main microbial groups used for the simulation of the anaerobic digestion process.

Group	μ_{max} (h^{-1})	K_s (g/L)
Undissolved carbohydrate-hydrolyzing bacteria	1.00	0.00
Undissolved protein-hydrolyzing bacteria	1.00	0.00
Glucose-fermenting acidogens	5.10	0.50
Lipolytic bacteria	0.53	0.01
LCFA-degrading acetogens	0.55	0.02
Amino acid-degrading acidogens	6.38	0.00
Propionate degraders	0.49	0.26
Butyrate degraders	0.67	0.18
Valerate-degrading acetogens	0.69	0.18
Aceticlastic methanogens	0.60	0.12

Adapted from Angelidaki et al. [40]. K_s : half-saturation constant; LCFAs: long-chain fatty acids; μ_{max} : maximum specific growth rate.

2.2. Techno-Economic Analysis

The techno-economic analysis of the process flowsheets was carried out using the SuperPro Designer simulator. The currency type used in the simulations was the United States dollar (\$). The direct fixed capital (DFC), equipment purchase cost (considering the equipment specifications and sizing), and purchase cost of plantain waste and utilities costs were calculated and consulted as described in previous works [8,34]. The techno-economic parameters (Table 2), list of equipment (Table 3), costs of other inputs, and selling price of products (outputs) (Table 4) considered during the assessment are shown as follows.

The labor force corresponding to each process flowsheet was calculated according to the definition in Colombia of a medium-sized company (51 workers) [43]. The labor base cost was estimated using the methodology described in previous works [8,34]. The labor quantity and its costs are shown in Table 5.

Table 2. Parameters used in the techno-economic assessment of the simulated process flowsheets.

Parameter	Value	Reference
Year of analysis	2020	
Year of construction start	2021	
Construction period (months)	12	
Start-up period (months)	2	
Project life (years)	15	
Inflation (%)	3.80	[44]
Rate of opportunity interest (for 2020) (%)	5.36	[45]
Depreciation: straight line (years)	10	
Salvage value fixed assets (% \times DFC)	5	
Income tax (% for 2020)	32	[46]
<i>Production volume of the plant</i>		
First year (%)	80	
Following years (%)	100	

DFC: direct fixed capital.

3. Results and Discussion

3.1. Process Development

3.1.1. Scale Definition and Data Collection

The definition of the scale for simulation of the SCP, NF, and BM processes was calculated from the information obtained from a plantain plantation in the experimental farm Montelindo at the Universidad de Caldas (Colombia) and using several forecasting methods as discussed in previous works [8,34]. The quantity of residues per year were estimated at 1,267,071 tons of pseudostems and 3179 tons of rejected unripe plantain fruits. These two types of residues were selected as independent feedstocks considering the utilization of *C. utilis* during the simulations that describe the SCP production. This yeast can assimilate 5- and 6-carbon sugars. For this reason, it is important to analyze each SCP process as a stand-alone process that utilizes either lignocellulosic materials (e.g., pseudostems) or starchy materials (e.g., the pulp of RUPFs) as feedstocks.

Table 3. Cost and specifications of the equipment used in the techno-economic assessment of the simulated process flowsheets.

Equipment Name	Equipment Type	Equipment Attribute ^{a,c}	Equipment Base Cost ^{a,b,f,g}	Base Cost Year ^a	Updated Equipment Cost (Year 2020)	Scaling Exponent ^{d,e}	Scaled Cost of Equipment
Belt washer	Washing (bulk flow)	8000 kg/h	\$ 11,445	2014	\$ 12,069	0.60	\$ 7962
Industrial blender	Grinding	1200 kg/h	\$ 3000	2014	\$ 3164	0.60	\$ 6515
Centrifugal pump	Fluid flow	16,000 kg/h	\$ 2397	2014	\$ 2528	0.58	\$ 2528
Flow distributor	Flow splitting	8000 kg/h	\$ 1450	2014	\$ 1529	0.48	\$ 2133
Valve solids and liquids	Mixing	8000 kg/h	\$ 3700	2014	\$ 3902	0.60	\$ 2574
Solid packed	Filling	1200 und/h	\$ 75,000	2018	\$ 75,547	0.60	\$ 75,547
Fermenter	Vessel procedure	50,000 L	\$ 35,000	2018	\$ 35,255	0.56	\$ 35,255
Fermenter	Seed fermentation	10,000 L	\$ 18,000	2014	\$ 18,981	0.56	\$ 18,981
Digester	Anaerobic digestion	50,000 L	\$ 42,500	2018	\$ 42,810	0.56	\$ 42,810
Balance tank	Storage	1000 L	\$ 1920	2014	\$ 2025	0.57	\$ 2025
Storage tank	Storage	10,000 L	\$ 19,800	2018	\$ 19,944	0.52	\$ 19,944
Plate and frame exchanger	Cooling/heating	8000 kg/h	\$ 7700	2014	\$ 8120	0.60	\$ 12,307
Centrifugal equipment	Centrifugation	16,000 kg/h	\$ 82,500	2018	\$ 83,102	0.67	\$ 83,102
Filter equipment (80 mesh)	Component splitting	8000 L	\$ 4100	2012	\$ 4261	0.59	\$ 6413
Decorticator	Shredding	150 kg/h	\$ 5500	2018	\$ 5540	0.60	\$ 5540

Gear pump	Fluid flow	2500 L/h	\$ 4900	2012	\$ 5092	0.34	\$ 5092
Mixing valve—liquids	Mixing	16,000 kg/h	\$ 1900	2012	\$ 1974	0.82	\$ 1974
Sterilize	Heat sterilization	5000 L/h	\$ 56,000	2014	\$ 59,052	0.60	\$ 118,666
Ion exchange equipment	Ion exchange	8000 L/h	\$ 16,000	2012	\$ 16,627	0.62	\$ 16,627
Dryer	Spray drying	86,000 L	\$ 82,500	2018	\$ 83,102	0.53	\$ 83,102
Dryer	Rotary drying	8000 L/h	\$ 9500	2014	\$ 10,018	0.60	\$ 10,018
Air compress	Gas compression	4000 kW	\$ 6500	2018	\$ 7767	0.69	\$ 7767
Solid conveyor	Screw conveying	D×L: 30 cm×5 m	\$ 4200	2014	\$ 4429	0.58	\$ 3293
Solid conveyor	Belt conveying	D×L: 30 cm×5 m	\$ 2900	2018	\$ 2921	0.58	\$ 1954
Condenser	Condensation	16,000 L/h	\$ 12,300	2012	\$ 12,782	0.79	\$ 12,782
Absorption column	Absorption	8000 L/h	\$ 15,500	2012	\$ 16,107	0.78	\$ 27,658
Degassing column	Degasification	8000 L/h	\$ 14,800	2012	\$ 15,380	0.78	\$ 26,409
Mechanical skinning	Shredding	150 kg/h	\$ 5200	2018	\$ 5238	0.60	\$ 5238
Microfiltration	Microfiltration	80 m ²	\$ 34,000	2018	\$ 34,248	0.60	\$ 34,248
Rotary drum filter	Rotary drum filter	80 m ²	\$ 30,000	2020	\$ 30,000	0.39	\$ 30,000

With information adapted from: ^a [47], ^b [48], ^c [49], ^d [50], ^e [51], ^f [52], ^g direct quotation. Inflation indices used in the escalation: 2014—576.1; 2018—603.1; 2019—607.5 [53]. D: diameter, L: length.

Table 4. Feedstock cost and selling price of products for 2020 used for the techno-economic assessment of the simulated process flowsheets.

Feedstock, Supplies and Utilities	Unit	Purchasing Price	References
Air ^a	\$/MT	5.362	
Electricity	\$/kWh	0.190	[54]
Gas	\$/m ³	0.650	[55]
Process water	\$/m ³	0.440	[56]
Cooling water ^a	\$/m ³	5.235	
Low pressure steam	\$/MT	7.560	[57]
Sodium hydroxide 50%	\$/kg	0.515	[58]
Sulfuric acid 98%	\$/kg	0.240	[58]
Nitric acid 68%	\$/kg	0.174	[58]
Ammonium sulfate	\$/kg	0.210	[58]
Ascorbic acid	\$/kg	2.700	[48]
Calcium chloride	\$/kg	0.200	[58]
HDPE	\$/kg	1.000	[48]
Cellulase	\$/kg	15.90	[48]
Hemicellulase	\$/kg	13.50	[48]
Amylogluosidase	\$/kg	20.00	[48]
Thermostable α -amylase	\$/kg	12.00	[48]
RUPF ^a	\$/kg	0.100	
Pseudostems and rachis ^a	\$/kg	0.052	
Products	Unit	Selling price	References
SCP	\$/kg	5.10	[8]
NF ^a	\$/kg	3.00	
BM	\$/m ³	1.20	
Sludge	\$/kg	0.10	

^a Average cost calculated from quotes provided by local and international companies. BM: bio-methane; HDPE: high-density polyethylene; NFs: natural fibers; RUPFs: rejected unripe plantain fruits; SCP: single-cell protein.

Table 5. Quantity and cost of labor used for the techno-economic assessment of the simulated processes.

Labor Type	Total Annual Salary (\$ per Person)	Persons
Plant manager	20,917	1
Secretary	6312	1
Plant engineer	18,702	3
Plant supervisor	14,765	3
Laboratory technician	8859	3
Maintenance technician	8859	3
Operators	7788	37
Total	86,202	51

On the other hand, during data collection from databases, 1715 papers and other published works were identified. From this amount, 343 were used and analyzed and the remaining ones discarded. These documents are related to different technological configurations for the SCP, NF, and BM production using different feedstocks, such as sugarcane, plantain, corn, wheat, and barley, among others.

3.1.2. Process Design and Simulation

The conceptual design of the studied processes was carried out from the analysis of the 343 documents obtained from the databases. These diagrams represent the basic structure of the different unit operations and unit processes intended for the conversion of the residues (pseudostems and RUPFs) into products. The conceptual design diagrams for single-cell protein production from plantain pseudostems and RUPFs (Figure 1), NF production from pseudostems (Figure 2), and BM production from pseudostems (Figure 3) are briefly described below.

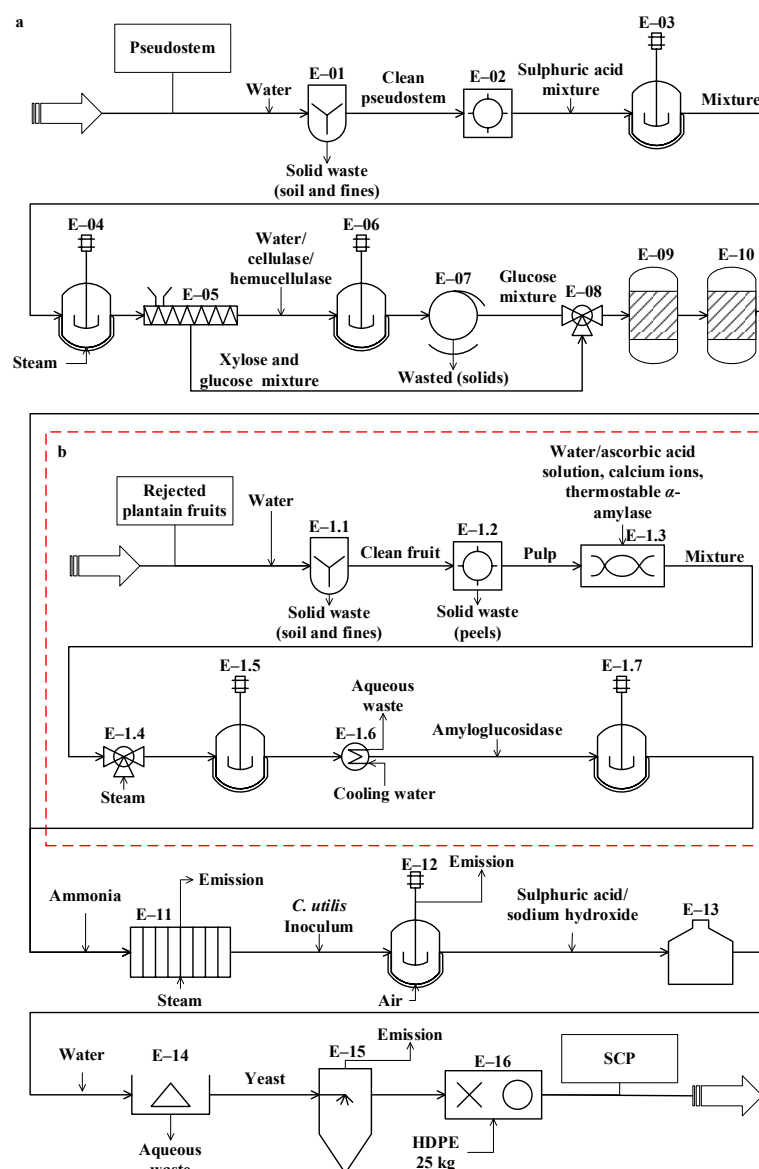


Figure 1. Diagram of the conceptual design for single-cell protein (SCP) production from (a) pseudostems and (b) rejected unripe plantain fruits.

The process proposed for SCP production from pseudostems (see Figure 1a) is described as follows. For washing (E-01), the plantain residues are immersed in water (3.5 m³ per ton) [59] at 25 °C in tanks with agitation for 12 min to remove other waste (soil and fines). For grinding (E-02), the residues are reduced in size down to particles between 1 and 2 mm. During the first pretreatment (E-03), the residues are mixed with sulfuric acid (2.2% v/v) [60]. The reaction is kept at 25 °C for 12 h with continuous stirring. In the second pretreatment (E-04), the mixture is treated by steam explosion at 177 °C for 5 min [60].

Then, the mixture is pressed (E-05) to extract the aqueous solution (90%) enriched with monosaccharides (mainly glucose and xylose).

For saccharification (E-06), water is added to the mixture and the pH is adjusted to 5.5 [61]. Cellulases and hemicellulases are added (6% and 2% w/v, respectively). The reacting mixture is continuously stirred at 45 °C for 24 h [61]. For filtration (E-07), the solids are removed through an 80-mesh filter. During the ion exchange (E-09 and E-10), the sugar mixture (E-08) is detoxified using H⁺ and OH⁻/Cl⁻ resins [62–64]. For sterilization (E-11), a solution containing 5 g/L ammonium sulfate is added to the mixture [65], which is heated at 121 °C for 15 min [15].

For fermentation (E-12), the sterilized culture medium is stored in reactors, and 10% *C. utilis* inoculum is added [15]. *C. utilis* was considered for fermentation due to its ability to assimilate different carbon sources, such as hexoses (e.g., glucose) and pentoses (e.g., xylose) [66,67]. In addition, this yeast is one of the most used for the production of SCP [10] and it is generally recognized as safe (GRAS) [68] for use in human food and animal feed. Then, the fermentation is kept under aerobic conditions at 30 °C and pH 4.5 for 24 h [69]. For the reduction of nucleic acids in yeast (E-13), the culture broth is mixed with concentrated sulfuric acid (12 mL/L); this procedure is needed in order to prevent the RNA from generating uric acid in the SCP consumer. Next, the acid-treated broth is heated at 80 °C for 30 min [70]. Afterwards, the broth is mixed with a solution of saturated sodium hydroxide up to pH 8.7 and the reaction is maintained for 10 min. For centrifugation (E-14), water is added to the resulting liquid stream continuously (at a rate of 1:1) and yeasts are separated by a disk-stack centrifuge [70]. Finally, the yeasts are dried to 150 °C in a spray dryer (E-15) [71], with a final moisture between 3% and 5% [72]. SCP is packed (E-16) in high-density polyethylene (HDPE) bags to obtain 25-kg packaged product units.

The process proposed in Figure 1b for SCP production from RUPFs is described as follows. For washing (E-1.1), the procedure briefly described above for unit E-01 is applied. For peeling (E-1.2), the peel is separated mechanically from pulp at a 150 kg/h flowrate. During grinding (E-1.3), the pulp is blended at 30,000 rpm for 10 min. In this step, 5% (w/v) ascorbic acid solution is added to the mixture to prevent enzyme damage [73]; then, total solids (TSs) are diluted up to 30% [74]. Next, 6 ppm calcium ions (as CaCl₂) per kilogram of mixture are added [75]. The mixture pH is adjusted to 5.5, and 0.15% (w/v) thermostable *Bacillus licheniformis* α -amylase liquid preparation is added [75]. For liquefaction (E-1.5), steam at 105 °C is mixed directly and continuously (jet cooking) (E-1.4) with the mixture [74]. The mixture temperature is adjusted up to 95 °C and kept under continuous stirring at 100 rpm for 3 h [75]. For saccharification (E-1.7), the pH and temperature of the mixture are adjusted to 4.5 and 60 °C (E-1.6), respectively, and 0.15 % (v/v) amyloglucosidase is added [76]. The hydrolysis is kept under continuous stirring in the reactors for 6 h. At the end of this step, the dextrose equivalent (DE) of the mixture must be greater than 80% [76]. Next, the procedures occurring in units E-11 to E-16 are applied (see Figure 1a).

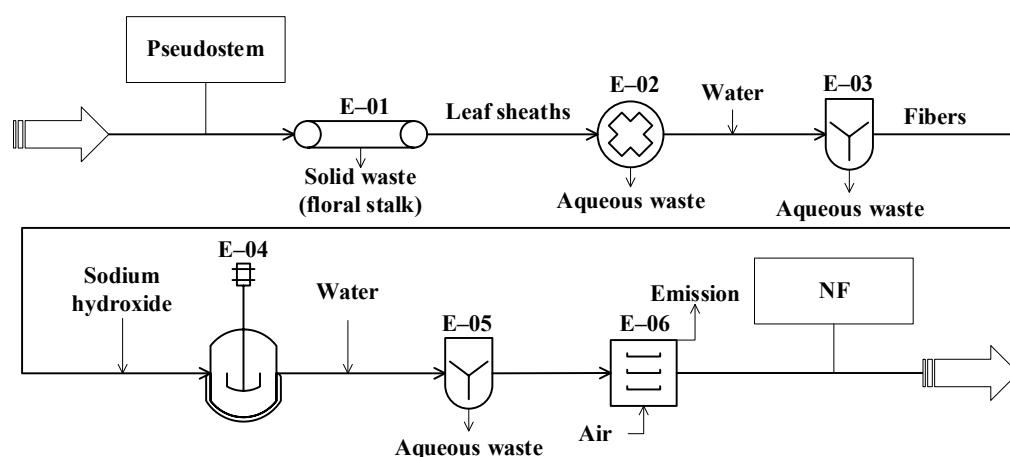


Figure 2. Diagram of the conceptual design for producing natural fibers (NFs) from pseudostems.

The process proposed to produce natural fibers (Figure 2) starts in the E-01 unit, where the leaf sheaths and floral stalk making up the pseudostems are mechanically separated. Then, the leaf sheaths are subjected to decortication (crus and bruise) using equipment with two cylinders (E-02) to extract the fibers [18]. Next, the fibers are washed (E-03) (water to fiber ratio of 2:1) to remove pigments and other compounds (part of fats, proteins, minerals, cellulose, hemicellulose, lignin, etc.). Then, the fibers are treated with 6% (w/v) sodium hydroxide (ratio of 2:1) (E-04). The reaction is kept in a tank with continuous stirring at 60 °C for 2 h [77,78]. During washing (E-05), the fibers are submerged in water (ratio of 2:1) at room temperature [18]. Finally, the fibers are dried (E-06) (maximum moisture of 8%) in a convection oven with air recirculation at 80 °C for 4 h [77].

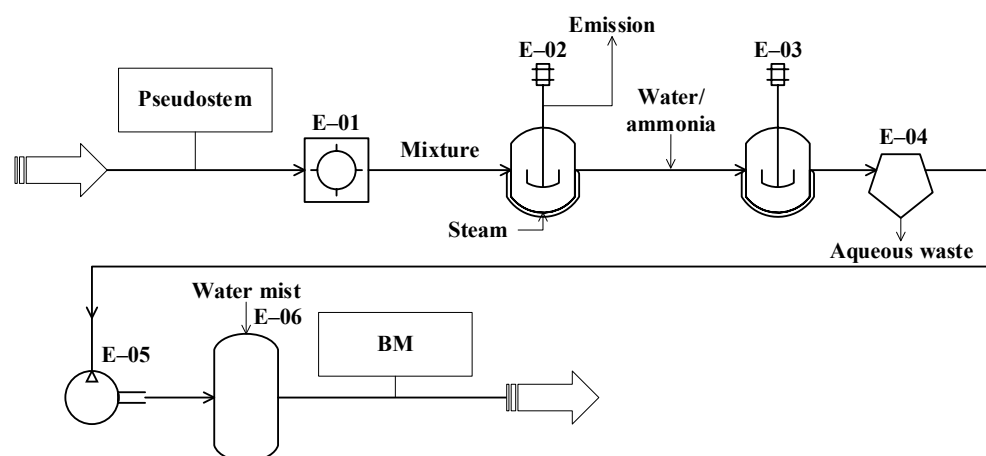


Figure 3. Diagram of the conceptual design for biomethane (BM) production from plantain pseudostems.

The process proposed for BM production from the pseudostems (see Figure 3) starts with the grinding operation (E-01), where the pseudostems are reduced in size down to particles between 1 and 2 mm. Then, the particles are pretreated (E-02) by steam explosion at 200 °C for 76 min [79]. The resulting mixture is dissolved with water down to 10%–15% TS [80]. During the anaerobic digestion (E-03), a solution containing 5 g/L ammonium sulfate is added to the mixture as a nitrogen source for the microorganisms. The process is performed under slow continuous stirring at 40 °C for 30 days [81]. For biogas cleaning, the water from gas is condensed and separated through a decanter (unit E-04) [81]. For desulphurization (E-06), the gas is compressed at 20 bar (E-05), then the gas is sent to an

absorption column (scrubber), where it is contacted with water mist to extract the carbon dioxide and hydrogen sulfide [81].

After building and describing the conceptual design (Figures 1–3), the first basic design of each one of the proposed processes was defined. The basic design of a process comprises a detailed analysis of the different unit operations and unit processes to define the process flowsheet, and information gathered from different sources used to simulate alternative operation modes [82,83]. In this way, the basic design includes the preparation of the process flowsheets, equipment list, corresponding mass and energy balances, and process scheduling (particularly important for batch processes). For this task, the SuperPro Designer simulator was employed in this work. In general, the basic design comprises all the documentation required to define the platform, production facility, and structure configurations and dimensions in satisfactory detail to allow the start of the detailed design (detailed engineering phase) [84].

The definition of the process flowsheets for the production of SCP, NFs, and BM started with the selection of the time regime of the whole process (batch vs. continuous). For this, the selected regime was batchwise due to the multiple sub-operations in the equipment, as discussed in previous works [8,34], and the technical impossibility of performing some processes in a continuous mode.

The following step to accomplish the basic design started from the conceptual design diagrams already built for the proposed processes. The analysis of these diagrams made it possible to identify which material streams are needed to connect the different unit procedures (e.g., through pumps, screws, etc.). The definition of these needs may affect the mass or volumetric flowrates of the different process streams, increasing the number of equipment units and affecting the techno-economic indicators. Therefore, for the process of SCP production from pseudostems, the equipment units for transferring solids (E-05, E-08, and E-13) and liquids (E-18, E-25, E-28, E-30, and E-35) and for balance storage (E-17 and E-34) were defined and included in the process flowsheet (see Figure 4). For SCP production from RUPFs, the equipment units for transferring liquids (E-09, E-12, E-15, E-21, E-24, E-26, and E-31) and for balance storage (E-08, and E-30) were included as well (Figure 5). For NF production, some units for transferring solids (E-03, E-10, and E-13) were added (Figure 6). Finally, for BM production, equipment units to transfer solids (E-02, E-04, and E-15) and liquids (E-06 and E-24), and for balance storage (E-05) were defined and added (Figure 7). The inclusion of these unit procedures allowed an assessment of their impact on the techno-economic index.

The basic design continued with the analysis of the input-output structure, according to Douglas' terminology [85]. The need to purify the feed streams before the transformation step (E-01 in Figure 1) made it possible to identify water recovery possibilities as an improvement of the design as discussed in previous works [8,34]. In this sense, for the processes of SCP production (Figures 4 and 5), a washing step (E-01) with a water recovery system (E-02) that separates the solids (soil and fines) and adjusts the flowrate with fresh water (E-03) was included. This variant made it possible to recover up to 90% of the water used in the washing step. For NF and BM production, there is no need to purify streams due to the nature of the processes, which do not require strict cleaning.

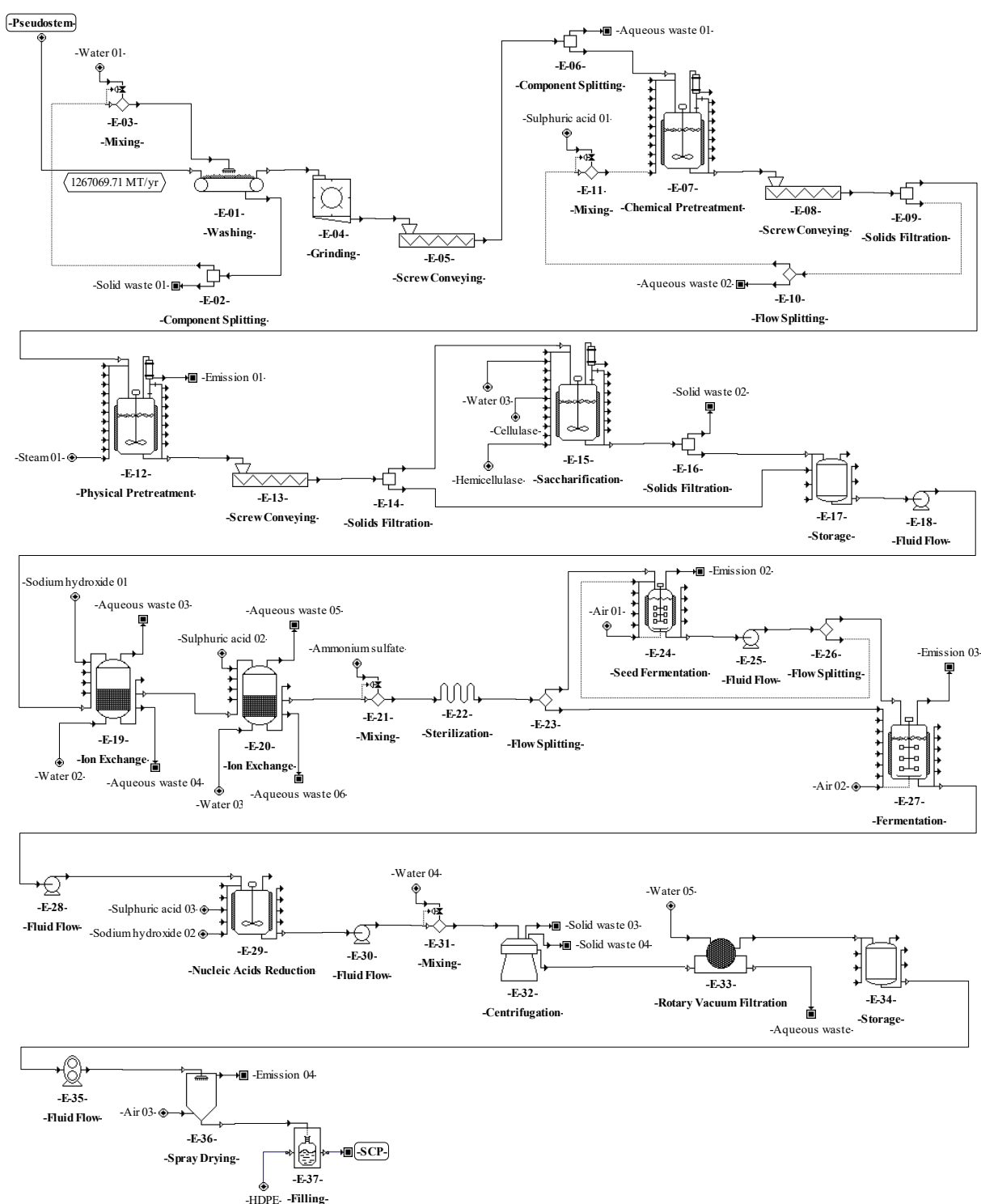


Figure 4. Process flowsheet of single-cell protein (SCP) production from plantain pseudostems.

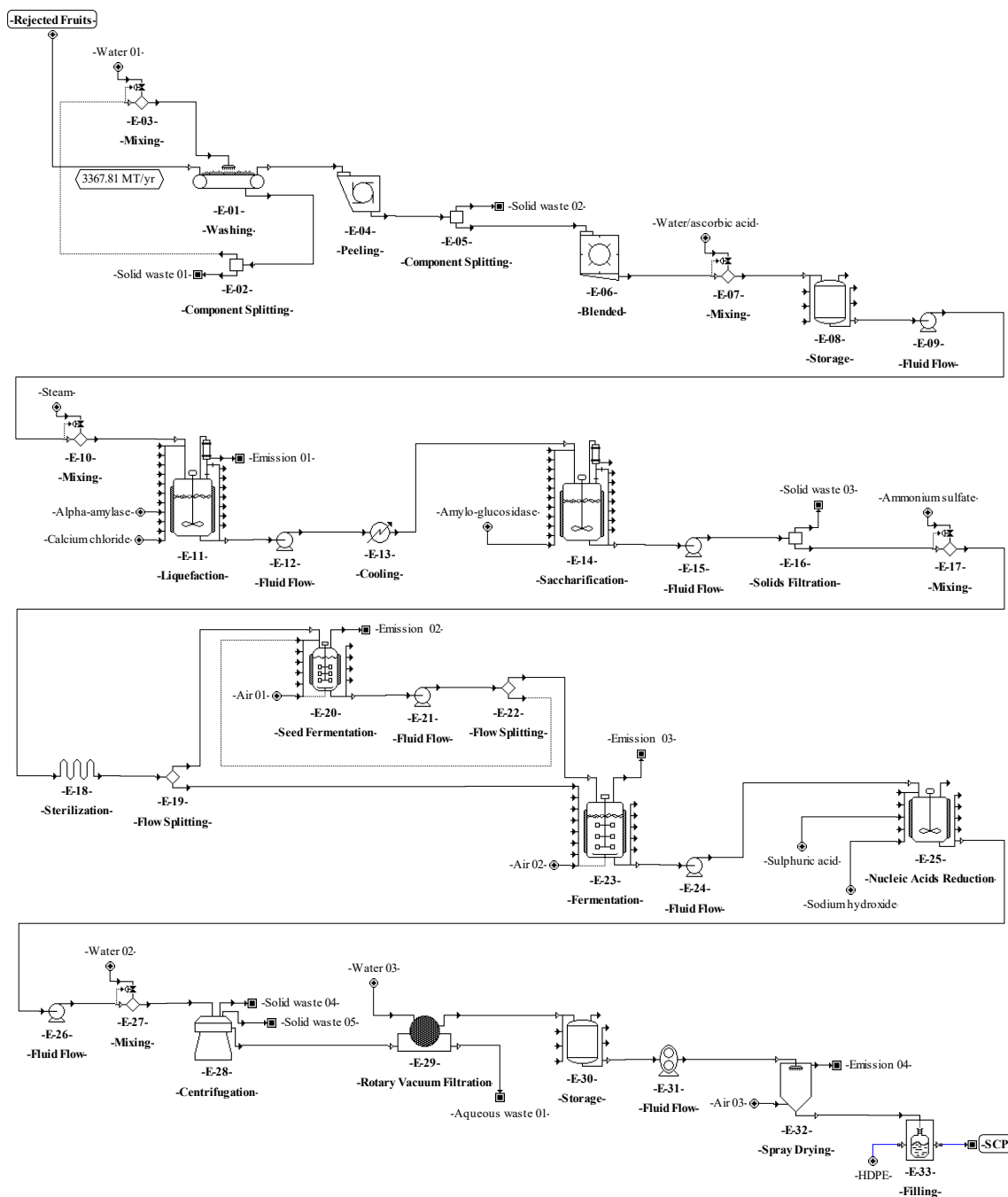


Figure 5. Process flowsheet of single-cell protein (SCP) production from rejected unripe plantain fruits.

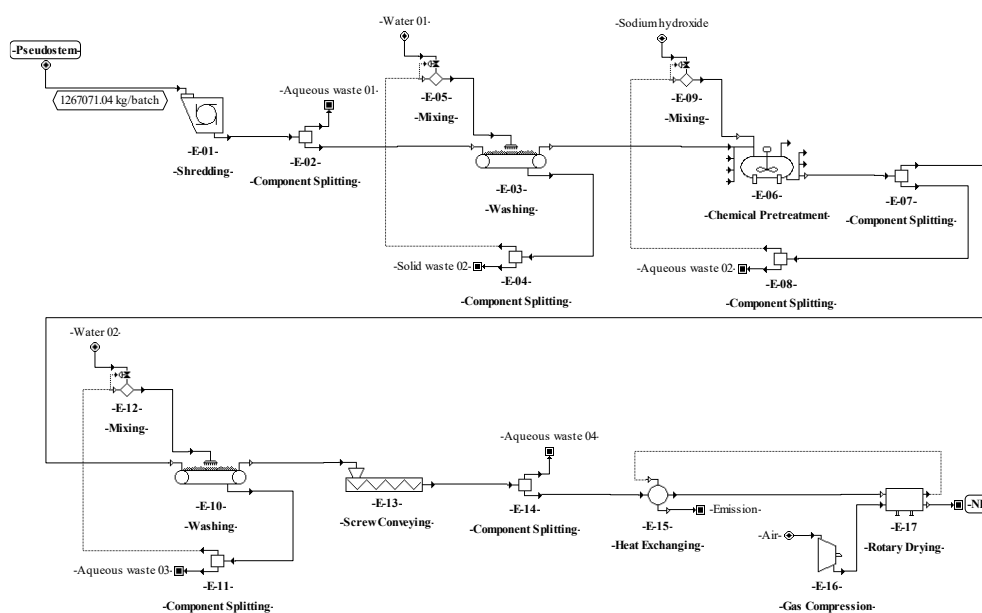


Figure 6. Process flowsheet of natural fiber (NF) production from plantain pseudostems.

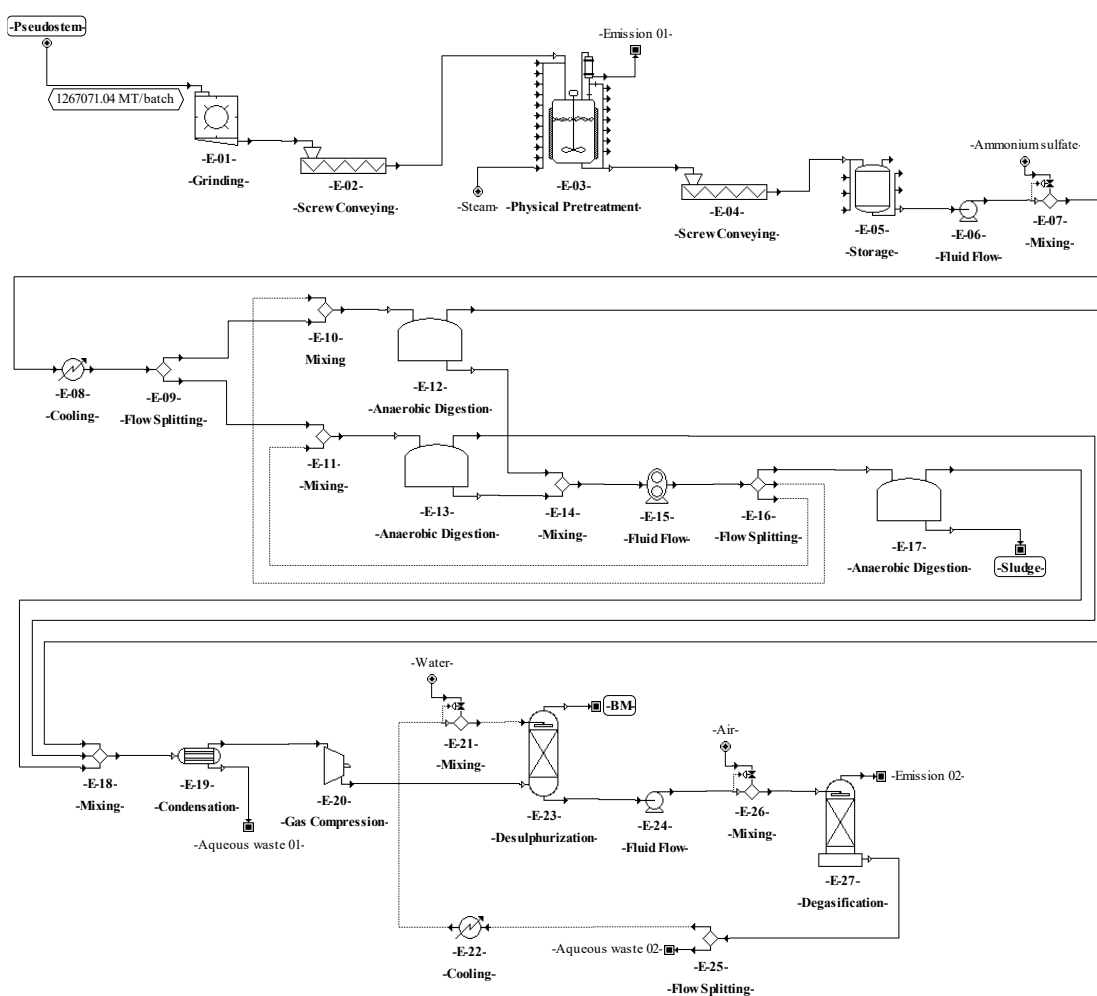


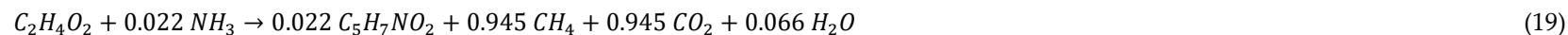
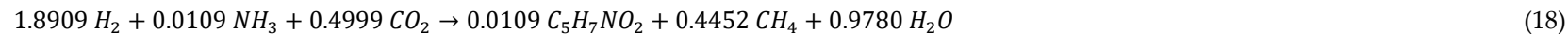
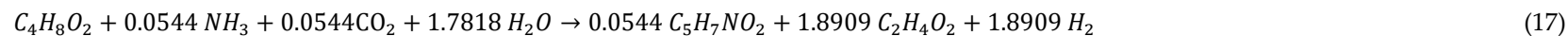
Figure 7. Process flowsheet of biomethane (BM) production from plantain pseudostems.

The preparation and definition of the process flowsheet also contemplated the analysis of the reaction system. The main transformations involved in the processes for producing SCP (aerobic cultivation) and BM (anaerobic digestion) are shown in Table 6. The reaction system corresponds to the recycle structure according to Douglas' terminology. In this sense, a recycle structure in the process flowsheet for SCP production from pseudostems (Figure 4) was included in the unit procedures E-24 to E-26. For SCP production from RUPFs, the recycle structure was added in the unit procedures E-20 to E-22 (Figure 5). The recycle structure in Figure 4 is described as follows: 10% of the sterilized mixture (E-23) is sent to the seed reactors (E-24), i.e., 10% of the *C. utilis* inoculum [15]. Fermentation is kept under aerobic conditions at 30 °C and pH 4.5 for 18 h [69]. At the end of this step, 30% of the volume of broth in the seed reactors is mixed in the main reactors (E-27) with 90% sterilized medium (E-23). Seventy percent of the broth volume (E-26) is recirculated to the seed reactors [69]. The recycle structure in Figure 5 was carried out in a similar way as in Figure 4. On the other hand, the process for NF production has no recycle structures (Figure 6). For the process of BM production (Figure 7), the recycle structure was added in the unit procedures E-10 to E-16. This system is described as follows: 30% of the sludge (E-16) is sent to the digesters for stabilization (E-17) and 70% is recirculated to the anaerobic digestion bioreactors (E-12 and E-13) [86], where it is mixed with fresh waste mixture (E-10 and E-11). The recycle structure in the fermentation or anaerobic digestion steps is paramount in the design of this type of biotechnological process since recirculation provides stability and improved performance by increasing the biomass concentration and reducing the conditioning time of the cultures in these steps [87].

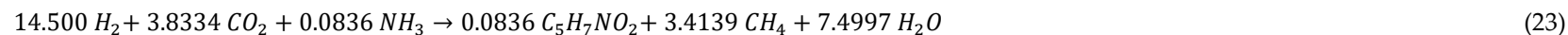
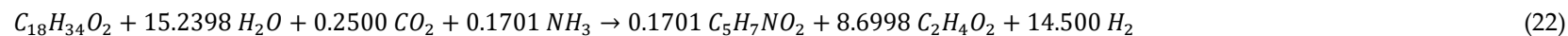
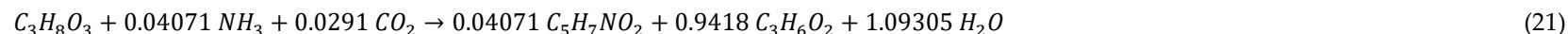
According to Douglas' methodology, the separation system is the next step during process design. In this regard, the separation of *C. utilis* from the broth was carried out through a disk-stack centrifuge and rotary vacuum filter (E-32 and E-33 in Figure 4, and E-28 and E-29 in Figure 5). Moreover, in this step, other separation schemes were analyzed as well. For instance, the chemical pretreatment (E-07 in Figure 4), a press system for solids (E-08) with acid solution recovery (E-09 and E-10), and flowrate adjustment (E-11) were included. This system allows the recovery of up to 90% of the aqueous solution. For the washing step (E-03 and E-10 in Figure 6), a recovery system of aqueous solution with solids separation (E-04 and E-11) and flowrate adjustment (E-05 and E-12) was also included. It is worth highlighting from this process the recovery of the aqueous solution (water and sodium hydroxide mixture) in the unit procedure E-07 and the inclusion of a hot air recovery step (E-15) that allows the recovery of up to 90% of air. This configuration provokes a temperature increase inside the fibers, decreasing the energy requirement during the subsequent drying. For the BM process, a water recovery system was implemented [88,89]. This system consists of a pump (E-24) that sends water under pressure from the desulphurization step (E-23) to the degasification step (E-27), where the water is mixed with air (E-26) to extract hydrogen sulfide and carbon dioxide. Then, the water is recovered (90%) (E-25), and the temperature (E-22) and flowrate (E-21) of this stream are adjusted.

Table 6. Reactions involved during the simulation of the process flowsheets for SCP and biomethane production.

Process	Steps	Reactions	Comments
SCP	Steam explosion (E-12) and saccharification (E-15) in Figure 4	From starch/cellulose to glucose	(5) Extent of the hydrolysis reaction of starch to glucose in the steam explosion step was assumed as 100%. Cellulose and hemicellulose hydrolysis was assumed as 19.4% and 90%, respectively [60]. Yield of reducing sugars (mainly glucose and xylose) in saccharification was assumed as 82% [90]. Reaction extent from starch to dextrin was 84.54 %, from dextrin to maltose was 63.27 %, and from dextrin to glucose was 36.72 % [8]. Reaction extent in saccharification was assumed as 80% [76].
		$C_{96}H_{162}O_{81} + H_2O \rightarrow 2C_{48}H_{82}O_{41}$	
		$C_{48}H_{82}O_{41} + 7H_2O \rightarrow 8C_6H_{12}O_6$	
		From hemicellulose to xylose	
	Liquefaction (E-11) and saccharification (E-14) in Figure 5	$C_{96}H_{162}O_{81} + H_2O \rightarrow 2C_{48}H_{82}O_{41}$	(7)
		$C_{48}H_{82}O_{41} + 7H_2O \rightarrow 9.6C_6H_{12}O_6$	(8)
	Fermentation (E-24 and E-27) in Figure 4 and (E-20 and E-23) in Figure 5	$C_6H_{12}O_6 + 2.0168 O_2 + 0.7734 NH_3$ $\rightarrow 3.8672 H_{1,84}O_{0,56}N_{0,2} + 2.1328 CO_2 + 3.6023 H_2O$	(9) Y_{xs} values were 0.55 g cells/g glucose [38] and 0.45 g cells/g xylose [91].
		$C_5H_{10}O_5 + 2.2842 O_2 + 0.5273 NH_3$ $\rightarrow 2.6367 CH_{1,84}O_{0,56}N_{0,2} + 2.3633 CO_2 + 3.3652 H_2O$	(10)
BM	Steam explosion (E-03)	From starch and cellulose to glucose	(11) Cellulose and hemicellulose hydrolysis was 19.4 % and 90 %, respectively [60].
		$C_6H_{10}O_5 + H_2O \rightarrow C_6H_{12}O_6$	
		From hemicellulose to xylose	
		$C_5H_8O_4 + H_2O \rightarrow C_5H_{10}O_5$	(12)
	Anaerobic digestion (E-12, E-13 and E-17)	Carbohydrate hydrolysis	
		$C_6H_{12}O_6 + 0.1115 NH_3 \rightarrow 0.1115 C_5H_7NO_2 + 0.7440 C_2H_4O_2 + 0.5000 C_3H_6O_2 + 0.4409 C_4H_8O_2 + 0.6909 CO_2 + 1.0254 H_2O$	(13)
$C_5H_{10}O_5 + 0.1115 NH_3 \rightarrow 0.1115 C_5H_7NO_2 + 0.2440 C_2H_4O_2 + 0.5000 C_3H_6O_2 + 0.4409 C_4H_8O_2 + 0.6909 CO_2 + 1.0254 H_2O$		(14)	
$C_3H_6O_2 + 0.0458 NH_3 + 1.764 H_2O \rightarrow 0.0458 C_5H_7NO_2 + 0.9345 C_2H_4O_2 + 2.804 H_2 + 0.902 CO_2$		(15)	
	$2.804 H_2 + 0.01618 NH_3 + 0.7413 CO_2 \rightarrow 0.01618 C_5H_7NO_2 + 0.6604 CH_4 + 1.45 H_2O$	(16)	

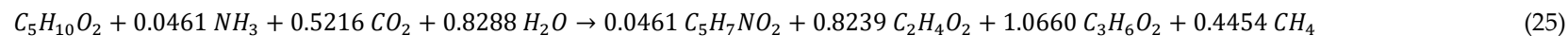
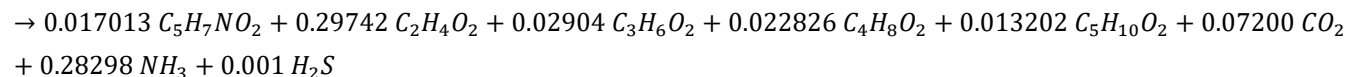


Lipid hydrolysis:



Reactions (15), (16), and (19) are subsequently applied.

Protein hydrolysis:



Reactions (15), (16), and (19) are subsequently applied.

Adapted from Angelidaki et al. [39,40] and Yu et al. [41].

Process simulation of the flowsheets performed as part of the basic design of the production of SCP, NFs, and BM allowed the calculation of the global mass balances and the process scheduling of each analyzed flowsheet at a large scale. The results obtained from the simulations are shown in Table 7.

Table 7. Overall process data and global mass balance for the simulated process flowsheets.

Item	Overall Process Data							
	SCP from Pseudostems		SCP from RUPF		NF from Pseudostems		BM from Pseudostems	
Tons (feedstock/batch)	5345		11.8		3661		115,145	
Production per year	643,317 units ^a /batch		2,352 units ^a /batch		41,746,712 kg/batch		18,227,294 m³/batch	
Batch size	2725 units		8.78 units		120,655 kg		5699 m³	
Batch time (h)	72		64		26		748	
Cycle time (h)	35		31		24		720	
Number of batches (year)	236		268		346		11	
Item	Bulk materials							
	SCP from pseudostems		SCP from RUPF		NF from pseudostems		BM from pseudostems	
	kg/year	%	kg/year	%	kg/year	%	kg/year	%
Air	886,941,554	20.57	2,801,926	24.83	254,841,101	14.87	19,749,496	1.13
Ammonium	4,347,546	0.10	7210	0.06		0.00	4,582,367	0.26
Amyloglucosidase		0.00	3046	0.03		0.00	0	0.00
Ascorbic acid		0.00	36,774	0.33		0.00	0	0.00
Calcium chloride		0.00	284	0.00		0.00	0	0.00
Cellulase	4,030,139	0.09		0.00		0.00	0	0.00
HDLPE	160,830	0.00	588	0.01		0.00	0	0.00
Hemicellulase	4,110,742	0.10		0.00		0.00	0	0.00
Pseudostems	1,261,515,615	29.26	0	0.00	1,266,874,890	73.92	1,151,458,715	65.74
RUPFs		0.00	3,166,598	28.06		0.00		0.00
Sodium hydroxide	22,795,261	0.53	34,511	0.31	16,313,776	0.95	0	0.00
Sulfuric acid	12,407,520	0.29	17,051	0.15		0.00	0	0.00
Thermostable α-amylase		0.00	4258	0.04		0.00	0	0.00
Water	2,115,234,498	49.06	5,211,804	46.19	175,904,450	10.26	575,759,358	32.87
Total	4,311,543,705	100.0	11,284,050	100.0	1,713,934,217	100.0	1,751,549,936	100.0

HDLPE: High-density polyethylene; BM: biomethane; NFs: natural fibers; RUPFs: rejected unripe plantain fruits; SCP: single-cell protein; ^a units: bags or containers weighing 25 kg.

The simulation results indicate that the process for NF production had the highest number of batches per year (346). This process had a recipe cycle time equal to the scheduled working time on each equipment (24 h). The results suggest that the productivity of the process was linked to the semi-continuous work of the equipment. This outcome can be verified from Figure 8, Figure 9, Figure 10, and Figure 11, where the equipment occupancy charts are presented. These charts show that some equipment units were scheduled to operate in parallel without waiting for the previous equipment to finish its operation. For example, in batch 1 (Figure 8), it is identified that all the equipment units are scheduled to start at the same time. This schedule enables the material flow entering the equipment to be processed in a semi-continuous mode to increase the amount of waste processed per unit of time.

On the other hand, the process for BM production had the lowest number of batches per year (11). This result is explained by the cycle time of this process, which reaches 30 days (720 h), especially the step of anaerobic digestion (E-12, E-13, and E-17 in Figure 11).

These equipment units represent the bottleneck of the process (recipe cycle time). The bottlenecks of the processes for the production of SCP (E-27 in Figure 8 and E-23 in Figure 9) and NFs (E-14 in Figure 10) were significantly lower.

The results presented in Table 6 also show that the processes demanding the highest amounts of bulk materials correspond to the production of SCP from pseudostems and natural fibers. This result is related to the batch size and the number of batches processed per year. The potential environmental impacts that the SCP and NF processes can have, are linked to the high energy and water consumption. The SCP production from RUPFs had a high consumption of air (24.83%) and water (46.19%). The air and water consumption in the NF process was 14.87% and 10.26%, respectively. The low water consumption in the NF process is explained by the inclusion of the water recovery system during the fiber washing.

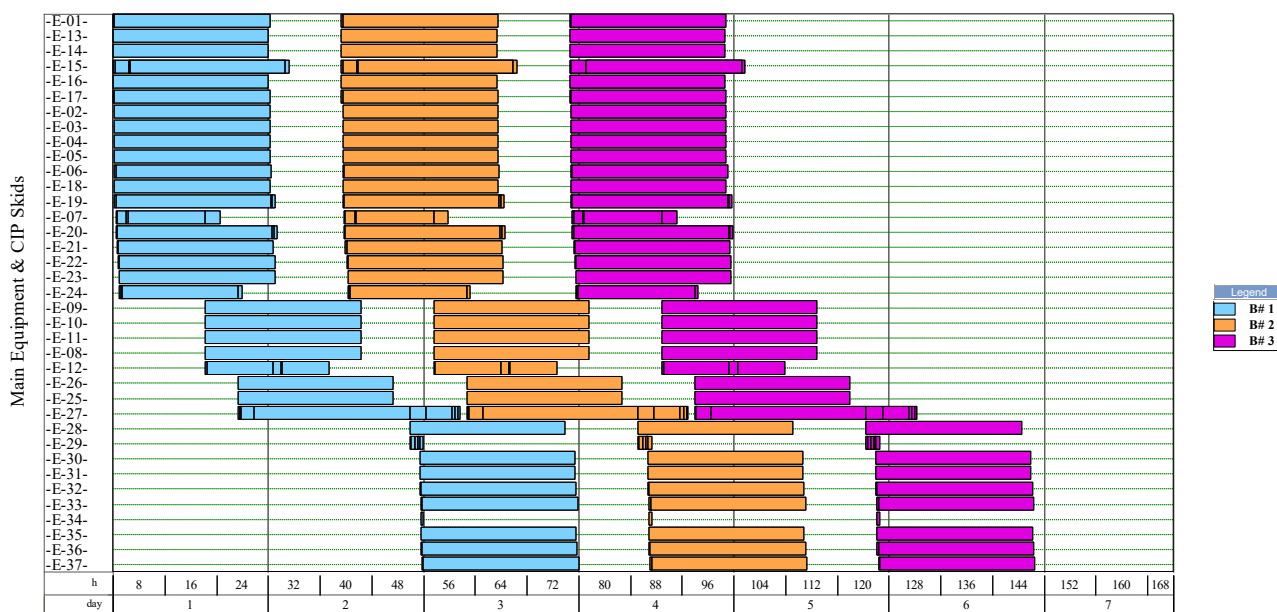


Figure 8. Equipment occupancy chart of the process for single-cell protein production from plantain pseudostems. B: batch; CIP: cleaning-in-place. The labels of the equipment units are shown in Figure 4.

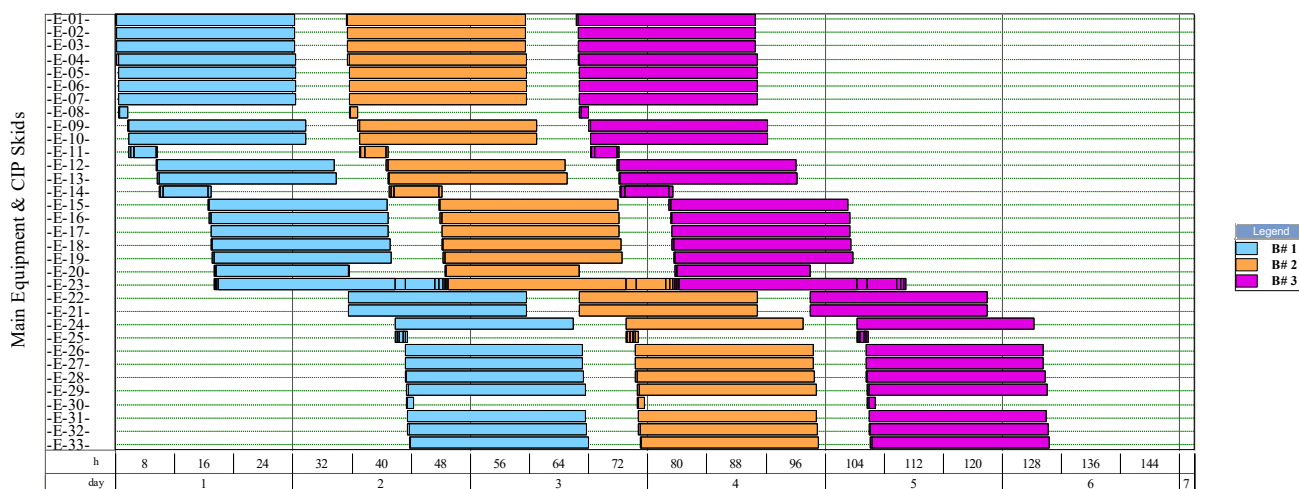


Figure 9. Equipment occupancy chart of the process for producing single-cell protein from rejected unripe plantain fruits. B: batch; CIP: cleaning-in-place. The labels of the equipment units are shown in Figure 5.

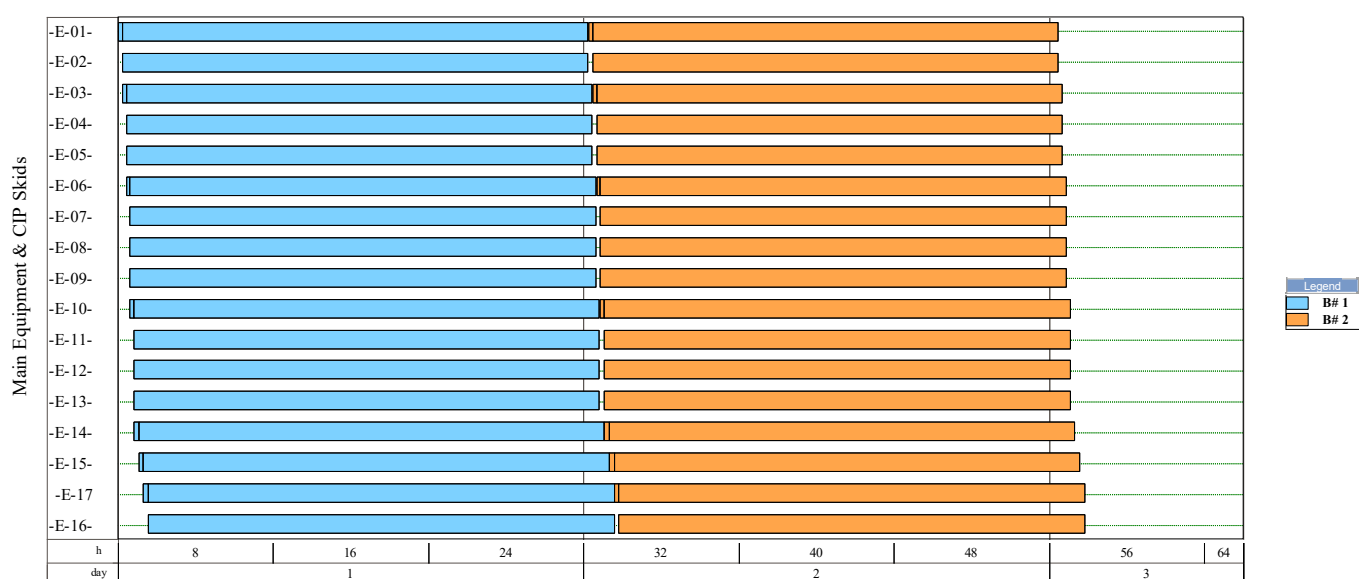


Figure 10. Equipment occupancy chart of the process for producing natural fibers from pseudostems. B: batch; CIP: cleaning-in-place. The labels of the equipment units are shown in Figure 6.

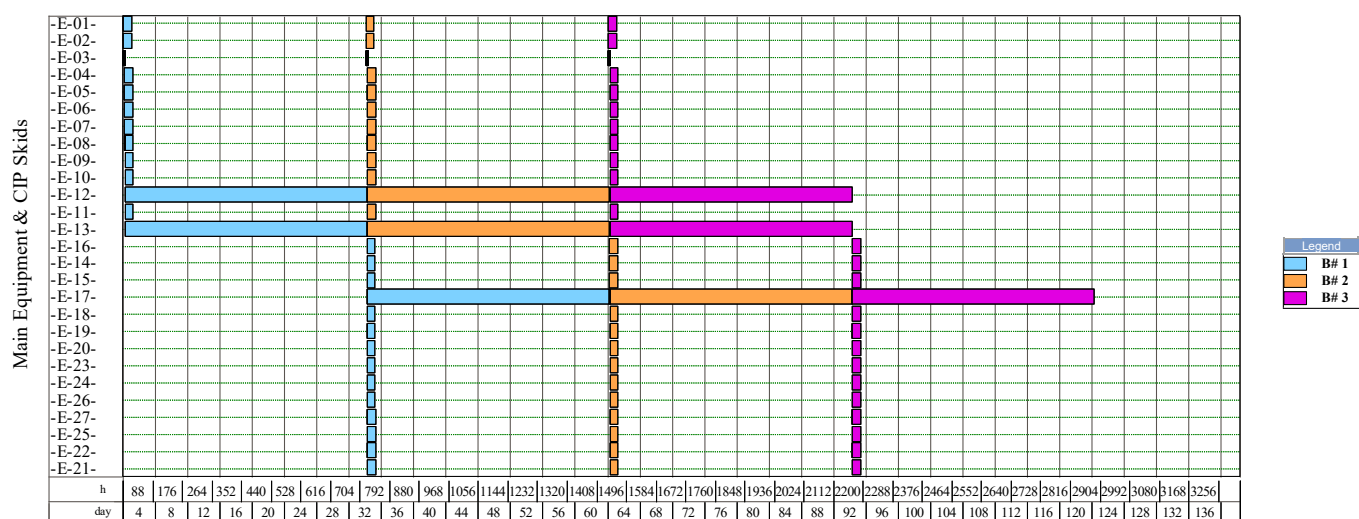


Figure 11. Equipment occupancy chart of the process for producing biomethane from pseudostems. B: batch; CIP: cleaning-in-place. The labels of the equipment units are shown in Figure 7.

3.2. Techno-Economic Analysis

A summary of the results of the techno-economic assessment as part of the basic design for the SCP, NF, and BM production processes is shown in Table 8. In addition, the unit operating and depreciation costs are presented in Table 9. The obtained results indicate that the process with the highest NPV corresponded to NF production (Figure 6). This process had 8.4% more income than its operating costs. Moreover, its direct fixed capital was lower than the other processes, not exceeding \$1,000,000. In this sense, the production of NF from plantain waste required a lower investment in equipment. For this process, AOCs were distributed as follows: 65.55% feedstocks, 0.40% labor, and 34.04% utilities. On the other hand, when comparing NPV of the process for NF production with NPV of other processes for the valorization of plantain waste, it is worth highlighting that NPV of NF was 48.8% higher than that of the process for the production of nutritional blocks for dairy cattle feeding reported in a previous work [34]. Likewise, the NF production process had NPV that is 98.43% higher than that of the process for the production of isomalto-

oligosaccharide syrup integrated with the production of single-cell protein from RUPFs, which has also been reported in a previous work [8]. In this sense, the NF process can be a profitable alternative for the valorization of plantain residues, especially for residual materials with a high fiber content such as pseudostems.

Table 8. Summary of the techno-economic assessment of the simulated process flowsheets.

Item	SCP from Pseudostems	SCP from RUPFs	NF from Pseudostems	BM from Pseudostems
Capital investment (\$)	56,581,000	2,633,000	17,352,000	99,894,000
Operating cost (\$)	112,775,000	2,029,652	115,534,965	169,497,695
Direct fixed capital (\$)	44,647,000	2,342,000	739,000	2,231,465,000
Income (\$)	50,074,000	300,000	125,240,000	109,711,000
Return on investment (%)	−110.82	−65.70	38.03	−59.85
Payback time (years)	NA	NA	2.63	NA
Internal rate of return (%)	NA	NA	50.39	NA
Net present value (\$)	−449,752,000	−13,465,000	29,299,000	−466,705,000

NA: Not applicable (parameter not calculated by the simulator). BM: Bio-methane; NFs: natural fibers; RUPFs: rejected unripe plantain fruits; SCP: single-cell protein.

The analysis of the results presented in Table 8 indicates that the selling prices of SCP (\$5.10 per kg) and BM (\$1.20 per m³) products were lower than the operating and depreciation costs per unit of products in 57.72% for SCP from RUPFs and 86.91% for SCP from pseudostems. In contrast, the selling price of NFs (\$3.00 per kg) was 62.33% higher than the unit operating and depreciation costs. According to these data, new configurations of the process flowsheets to reduce production costs were analyzed. These configurations implied the elimination of the washing steps, extraction of water from the waste through pressing, and reduction in labor. Thus, for the SCP process that employs pseudostems, the equipment units E-01, E-02, and E-03 were eliminated. For the SCP process that uses RUPFs, equipment units E-01, E-02, and E-03 were also eliminated and the labor was reduced to 17 workers. For the SCP and BM processes from pseudostems, 70% moisture was removed from the feedstock (E-05 and E-02). These configurations were proposed since the analysis of the direct fixed capital cost and the annual operating cost showed that the simulation of the original process for SCP production from pseudostems resulted in an exaggerated amount of equipment units (up to 1000 units of the same equipment E-03 in Figure 7) to process the entering amount of residues. On the other hand, labor in the SCP process from RUPFs was lower because the batch size (3179 tons) was smaller than that of the SCP process from pseudostems (1,267,071 tons).

Table 9. Operating and depreciation costs per unit of products for the simulated process flowsheets.

Item	SCP from Pseudostems	SCP from RUPFs	NF from Pseudostems	BM from Pseudostems
Feedstocks (\$ per pack)	8.736	10.442	1.814	0.073
Labor (\$ per pack)	0.048	7.942	0.011	0.001
Consumables (\$ per pack)	0.006	0.000	0.000	0.000
Utilities (\$ per pack)	2.697	16.122	0.011	0.116
Capital depreciation (\$ per pack)	0.576	4.478	0.042	0.011
Total	12.062	38.985	1.878	0.200

BM: biomethane; NFs: natural fibers; RUPFs: rejected unripe plantain fruits; SCP: single-cell protein.

After performing the corresponding simulations, the implemented modified configurations increased NVP of the SCP and BM processes but not enough to reach a value greater than 0. For SCP from pseudostems, NPV was \$−89,657,441; for SCP from RUPFs, it was \$−9,066,821; and for BM production from pseudostems, it was \$−188,595,941. The process for NF production was not modified considering that its NPV was profitable. It is evident from these results that this type of process, independently implemented for a large scale (stand-alone processes), is not techno-economically profitable under the analyzed context, except for the case of NF production. An alternative to improve the profitability of such processes that have NPV lower than 0 may be its integration into a biorefinery that valorizes the residues from the plantain agro-industry in an integral way. In this sense, lignocellulosic and starchy waste can be precursors of different products that, due to their variety, can provide different cash flows, directly impacting NPV of the biorefinery. Thus, the internal rate of return (IRR) of such a biorefinery process could approach the typical profit margin of the production processes intended to obtain miscellaneous fabricated products worldwide, which is about 5.03% [92]. In this potential case, the profitability of this type of biorefinery could be attractive for potential investors.

3.3. Integration Possibilities of the Simulated Processes in a Biorefinery

Biorefineries are sustainable industrial structures that recover the most compounds, especially carbon from residual biomass, in a wide portfolio of products, such as food, feed, biofuels, and energy [93]. Biorefineries are composed of different platforms that allow efficient and sustainable connection of feedstocks with products [9]. Thus, biorefineries are presented as facilities of the future that integrate multiple processes synergistically to benefit the environment and society.

The implementation of each of the processes simulated in this work into the design of a second-generation biorefinery may lead to processing of most of the residues from the plantain agro-industry. In addition, the possibilities of processing each one of the analyzed residues in a separate way (pseudostems and rejected unripe plantain fruits) can increase the profitability of the integrated processes. Moreover, the simulated processes (profitable and unprofitable) could be the basis for integrating them into the design of a biorefinery because they provide technological configurations that become alternative processing routes for a biorefinery that utilizes such residues. In addition, the products whose production was simulated in this work are non-traditional products, different from the products that are analyzed in most published papers dealing with biorefinery design, such as biofuels (e.g., bioethanol), furfural, xylitol, or animal feed. In this sense, it is necessary to design biorefineries for the processing of lignocellulosic and starchy materials contained in the residues of the plantain agro-industry (pseudostems and RUPFs, among others).

The integration of each of the processes simulated in this work, and other valorization processes studied in previous works [8,34], into the design of a multi-input second-generation biorefinery can lead to the sustainable valorization of all residues generated in the plantain agro-industry. Plantain residues are formed by different materials that can

potentially be used (with an appropriate prior separation) to obtain two valuable streams: lignocellulosic and starchy streams. These streams can be directed into two different processing pathways of the biorefinery design. For instance, the pulp of RUPFs (starchy stream) can be used to obtain SCP, whereas natural fibers can be obtained from plantain pseudostems (lignocellulosic stream). The integration of these processes is subject to the unit operations and unit processes that make up the platforms to be considered during the biorefinery design. Therefore, it is necessary to generate and implement methodological approaches to design biorefineries under these conditions, considering the particularity of the use of starchy and lignocellulosic materials. In this way, waste reduction and economic growth in rural communities could be accomplished simultaneously. Regarding this, such a design procedure for these facilities will be explored in future work.

4. Conclusions

Different processes for the valorization of waste from the plantain agro-industry (production of SCP, NFs, and BM) were designed and techno-economically assessed using process simulation tools. The results indicate that the operating costs (specifically, the consumption of utilities such as energy and water) and the quantity of obtained products are decisive factors in the profitability of these processes. In this sense, the scale and quantity of batches processed per year may affect the profitability of these types of processes on different scales of operation. In particular, processes with an extensive bottleneck such as the one for biomethane production can be disadvantageous in economic terms when included in the design of a future biorefinery processing plantain agro-industry waste.

On the other hand, the initial classification and separation of plantain residues into two streams (lignocellulosic and starchy materials) can help define the capacity and improve the profitability of these valorization processes in order to be integrated into a biorefinery. Such separation may offer the possibility of producing higher-value-added products, such as prebiotic compounds, among others, which could not be obtained if the two types of streams are mixed from the beginning of the corresponding process flowsheets. For this, a design methodology or design framework should be developed for this type of multi-input second-generation biorefinery. This issue will be addressed in future work. In addition, it is also necessary to analyze the supply chain of residues from the plantain agro-industry to determine its optimal availability and periodicity of harvest for a specific location to ensure proper operation of the valorization processes analyzed in this work throughout the year.

Author Contributions: J.A.G.: conceptualization, methodology, formal analysis, investigation, software, and writing—review and editing. L.G.M.: software, formal analysis, and editing. Ó.J.S.: conceptualization, formal analysis, writing—review and editing, validation, and supervision. All authors have read and agreed to the published version of the manuscript.

Funding: This work was supported by the Colombian Ministry for Science, Technology, and Innovation (MinCiencias) through the research project “Design of a Biorefinery for the Use of the Lignocellulosic and Starchy Waste of the Plantain Agribusiness” (Call 757 for Funding of National Doctorates) [grant 1640318]; and the Universidad de Caldas through the research project “Basic Process Development for the Use of Agro-industrial and Urban Waste Under the Concept of Biorefineries” [grant 0240518].

Institutional Review Board Statement: Not applicable.

Informed Consent Statement: Not applicable.

Data Availability Statement: Not applicable.

Acknowledgments: James A. Gómez S. acknowledges the Colombian Ministry of Science, Technology and Innovation of Colombia (MinCiencias) for the financial support to carry out this work and the Faculty of Engineering at the Universidad de Caldas for its financial and administrative assistance.

Conflicts of Interest: The authors declare no conflict of interest.

References

1. Coral-Velasco, D.A.; Correa, L.F.; Sánchez, Ó.J.; Gómez, J.A. Process design and techno-economic assessment of cellulolytic enzymes production from coffee husk through process simulation. *Biomass Convers. Biorefin.* **2022**, *https://doi.org/10.1007/s13399-022-03130-8*.
2. FAO. FAOSTAT: Food and Agriculture Data. Available online: <http://www.fao.org/faostat/es/#data> (accessed on 2 February 2022).
3. Escalante, H.; Orduz, J.; Zapata, H.; Cardona, M.; Duarte, M. *Atlas del Potencial Energético de la Biomasa Residual en Colombia (Atlas of the Energy Potential of the Residual Biomass in Colombia)*; Unidad de Planeación Minero Energética; IDEAM Colciencias, Universidad Industrial de Santander: Bogotá, Colombia, 2009; p. 182.
4. Blanco, G.; Linares, B.; Hernández, J.; Maselli, A.; Rincón, A.; Ortega, R.; Medina, E.; Hernández, L.; Morillo, J. Caracterización química de lixiviados de pseudotallos y láminas foliares de plátano “Hartón” en el estado Yaracuy (Chemical characterization of leachates pseudostems and leaf blades of ‘Hartón’ plantain in Yaracuy state). *Agron. Trop.* **2013**, *63*, 121–134.
5. Gómez, J.; Sánchez, Ó.; Matallana, L. Procesos de transformación: perspectiva de aprovechamiento para los residuos de la agroindustria del plátano (Processes of transformation: perspective of use for the residues of the plantain agro-industry). *Rev. P+L* **2021**, *16*, 6–30. <https://doi.org/10.22507/pml.v16n1a1>.
6. Gómez, J.; Sánchez, Ó.; Matallana, L. Residuos urbanos, agrícolas y pecuarios en el contexto de las biorrefinerías (Urban, agricultural and livestock waste in the context of biorefineries). *Rev. Fac. Ing.* **2019**, *28*, 7–32. <https://doi.org/10.19053/01211129.v28.n53.2019.9705>.
7. Gómez, J.; Pino, E.; Abrunhosa, L.; Matallana, L.; Sánchez, Ó.; Teixeira, J.; Nobre, C. Valorisation of rejected unripe plantain fruits of *Musa AAB* Simmonds: from nutritional characterisation to the conceptual process design for prebiotic production. *Food Funct.* **2021**, *12*, 3009–3021. <http://dx.doi.org/10.1039/D0FO03379K>.
8. Gómez, J.; Berni, P.; Matallana, L.; Sánchez, Ó.; Teixeira, J.; Nobre, C. Towards a biorefinery processing waste from plantain agro-industry: process development for the production of an isomalto–oligosaccharide syrup from rejected unripe plantain fruits. *Food Bioprod. Process.* **2022**, *133*, 100–118. <https://doi.org/10.1016/j.fbp.2022.03.005>.
9. de Jong, E.; Higson, A.; Walsh, P.; Wellisch, M. *Bio-based chemicals. Value added products from biorefineries*; IEA Bioenergy: Wageningen, The Netherlands, 2012; 34 p.
10. Bajpai, P. Microorganisms used for single-cell protein production. In *Single Cell Protein Production from Lignocellulosic Biomass*; Bajpai, P., Ed.; Springer: Singapore, 2017; pp. 21–30.
11. Awais, H.; Nawab, Y.; Amjad, A.; Anjang, A.; Md Akil, H.; Zainol Abidin, M. Environmental benign natural fibre reinforced thermoplastic composites: A review. *Composites Part C: Open Access* **2021**, *4*, 100082. <https://doi.org/10.1016/j.jcomc.2020.100082>.
12. Bismarck, A.; Mishra, S.; Lampke, T. Plant fibers as reinforcement for green composites. In *Natural Fibers, Biopolymers, and Biocomposites*; Mohanty, A.; Misra, M.; Drzal, L., Eds.; CRC Press: Boca Raton, FL, United States, 2005; pp. 51–122.
13. EPA. Basic information about anaerobic digestion (AD). Available online: <https://n9.cl/0j3bm> (accessed on 20 November 2021).
14. Adoki, A. Factors affecting yeast growth and protein yield production from orange, plantain and banana wastes processing residues using *Candida* sp. *Afr. J. Biotechnol.* **2008**, *7*, 290–295.
15. Pujol, F.; Bahar, S. Production of single cell protein from green plantain skin. *Eur. J. Appl. Microbiol. Biotechnol.* **1983**, *18*, 361–368. <https://doi.org/10.1007/BF00504746>.
16. Alsudani, A. Production of polysaccharides and single-cell protein by some local isolates of *Trichoderma* spp. *Pak. J. Biol. Sci.* **2021**, *24*, 971–977. <https://doi.org/10.3923/pjbs.2021.971.977>.
17. Aker, K.; Robinson, C. Growth of *Candida utilis* on single and multicomponent–sugar substrates and on waste banana pulp liquors for single-cell protein production. *MIRCEN J. Appl. Microbiol. Biotechnol.* **1987**, *3*, 255–274. <https://doi.org/10.1007/BF00933579>.
18. Cadena, E.; Vélez, M.; Santa, J.; Otálvaro, V. Natural fibers from plantain pseudostem (*Musa paradisiaca*) for use in fiber-reinforced composites. *J. Nat. Fibers* **2017**, *14*, 678–690. <https://doi.org/10.1080/15440478.2016.1266295>.
19. Gañán, P.; Zuluaga, R.; Restrepo, A.; Labidi, J.; Mondragon, I. Plantain fibre bundles isolated from Colombian agro-industrial residues. *Bioresour. Technol.* **2008**, *99*, 486–491. <https://doi.org/10.1016/j.biortech.2007.01.012>.
20. Awedem, F.; Happi, T.; Fokou, E.; Boda, M.; Gillet, S.; Deleu, M.; Richel, A.; Gerin, P. Comparative biochemical methane potential of some varieties of residual banana biomass and renewable energy potential. *Biomass Convers. Biorefin.* **2017**, *7*, 167–177. <https://doi.org/10.1007/s13399-016-0222-x>.
21. Miezah, K.; Obiri, K.; Kádár, Z.; Heiske, S.; Fei, B.; Mensah, M.; Meyer, A. Municipal solid waste management in a low income economy through biogas and bioethanol production. *Waste Biomass Valorization* **2017**, *8*, 115–127. <http://10.1007/s12649-016-9566-5>.
22. Ezekoye, V.; Ezekoye, D.; Ofomatah, A.; Agbaogu, A. Comparative study of calorific values and proximate analysis of biogas from different feedstocks. In *IOP Conference Series: Earth and Environmental Science*, Proceedings of the 4th International Conference/Training Workshop on Energy for Sustainable Development in Africa, ICTWESDA 2020, Nsukka, Nigeria, 11–13 November, 2020; IOP Publishing, 2021; 17 p.
23. Alonso, L.; Solarte, J.; Bello, L.; Cardona, C. Performance evaluation and economic analysis of the bioethanol and flour production using rejected unripe plantain fruits (*Musa paradisiaca* L.) as raw material. *Food Bioprod. Process.* **2020**, *121*, 29–42. <https://doi.org/10.1016/j.fbp.2020.01.005>.

24. Elahi, M.; Yusuf, A.; Torshabi, A.; Fazaeli, H.; Dehghani, M.; Salem, A. Ensiling pretreatment of banana waste by-products: Influences on chemical composition and environmental rumen biogas and fermentation. *Waste Biomass Valorization* **2019**, *10*, 3363–3371. <https://doi.org/10.1007/s12649-018-0312-z>.
25. Xue, Z.; Mu, L.; Cai, M.; Zhang, Y.; Wanapat, M.; Huang, B. Effect of using banana by-products and other agricultural residues for beef cattle in southern China. *Trop. Anim. Health Prod.* **2020**, *52*, 489–496. <https://doi.org/10.1007/s11250-019-02031-9>.
26. Monteiro, H.; Paula, E.; Muck, R.; Broderick, G.; Faciola, A. Effects of lactic acid bacteria in a silage inoculant on ruminal nutrient digestibility, nitrogen metabolism, and lactation performance of high-producing dairy cows. *J. Dairy Sci.* **2021**, *104*, 8826–8834. <https://doi.org/10.3168/jds.2021-20155>.
27. Godoy, D.; Puémape, F.; Roque, R.; Fernández, M.; Vargas, J.; Gamarra, S.; Hidalgo, V.; Gómez, C. Efecto de la suplementación de bloques multinutricionales con residuos agroindustriales en la producción y calidad de leche de vacas criollas al pastoreo en San Martín, Perú (Effect of the supplementation of multi-nutritional blocks with agro-industrial by-products on the production and quality of milk of criollo cows at grazing in San Martín, Peru). *Rev. de Investig. Vet. del Peru* **2020**, *31*, e19029. <http://dx.doi.org/10.15381/rivep.v31i4.19029>.
28. Suárez, D.; Marín, O.; Ortiz, J.; Puentes, A.; Ballesteros, L.; Suárez, M. Biotechnology as a tool for the agroindustrial exploitation of residues of the chain of *Musa* spp. *Chem. Eng. Trans.* **2018**, *64*, 571–576. <https://doi.org/10.3303/CET1864096>.
29. Windsor, P.; Martin, S.; Khounsy, S.; Young, J.; Thomson, P.; Bush, R. Improved milk production from supplementation of swamp buffalo with molasses nutrient blocks containing 10% urea. *Dairy* **2021**, *2*, 90–103. <https://doi.org/10.3390/dairy2010009>.
30. de Evan, T.; Carro, M.; Fernández, J.; Haro, A.; Arbesú, L.; Romero, M.; Molina, E. Effects of feeding multinutrient blocks including avocado pulp and peels to dairy goats on feed intake and milk yield and composition. *Animals* **2020**, *10*, 194. <https://doi.org/10.3390/ani10020194>.
31. Baidhe, E.; Kigozi, J.; Mukisa, I.; Muyanja, C.; Namubiru, L.; Kitarikawe, B. Unearthing the potential of solid waste generated along the pineapple drying process line in Uganda: A review. *Environ. Challenges* **2021**, *2*, 100012. <https://doi.org/10.1016/j.envc.2020.100012>.
32. Aboudi, K.; Fernández, L.; Álvarez, C.; Romero, L. Biogas, biohydrogen, and polyhydroxyalkanoates production from organic waste in the circular economy context. In *Sustainable Biofuels*; Ray, R., Ed.; Academic Press: Cambridge, MA, United States, 2021; pp. 305–343.
33. Morsetto, P. Targets for a circular economy. *Resour. Conserv. Recycl.* **2020**, *153*, 104553. <https://doi.org/10.1016/j.resconrec.2019.104553>.
34. Gómez, J.; Nobre, C.; Teixeira, J.; Sánchez, Ó. Towards a biorefinery processing waste from plantain agro-industry: assessment of the production of dairy cattle feed through process simulation. *Biosys. Eng.* **2022**, *217*, 131–149. <https://doi.org/10.1016/j.biosystemseng.2022.03.008>.
35. ISO. *ISO 10628-1:2014; Diagrams for the chemical and petrochemical industry – Part 1: Specification of diagrams*. International Organization for Standardization (ISO): Geneva, Switzerland, 2014; 16 p.
36. Wyman, C.; Decker, S.; Himmel, M.; Brady, J.; Skopec, C.; Viikari, L. Hydrolysis of cellulose and hemicellulose. In *Polysaccharides: Structural Diversity and Functional Versatility*; Dumitriu, S., Ed.; Marcel Dekker: New York, NY, USA, 2005; pp. 1013–1051.
37. Doran, P. *Bioprocess Engineering Principles*; Academic Press: Oxford, UK, 2013.
38. Tobajas, M.; García, E.; Wu, X.; Merchuk, J. A simple mathematical model of the process of *Candida utilis* growth in a bioreactor. *World J. Microbiol. Biotechnol.* **2003**, *19*, 391–398. <https://doi.org/10.1023/A:1023942602041>.
39. Angelidaki, I.; Ellegaard, L.; Ahring, B. A mathematical model for dynamic simulation of anaerobic digestion of complex substrates: Focusing on ammonia inhibition. *Biotechnol. Bioeng.* **1993**, *42*, 159–166. <https://doi.org/10.1002/bit.260420203>.
40. Angelidaki, I.; Ellegaard, L.; Ahring, B. A comprehensive model of anaerobic bioconversion of complex substrates to biogas. *Biotechnol. Bioeng.* **1999**, *63*, 363–372. [https://doi.org/10.1002/\(SICI\)1097-0290\(19990505\)63:3<363::AID-BIT13>3.0.CO;2-Z](https://doi.org/10.1002/(SICI)1097-0290(19990505)63:3<363::AID-BIT13>3.0.CO;2-Z).
41. Yu, L.; Wensel, P.; Ma, J.; Chen, S. Mathematical modeling in anaerobic digestion (AD). *J. Biorem. Biodegrad.* **2013**, *54*, 1–12. <https://doi.org/10.4172/2155-6199.S4-003>.
42. Diwekar, U. *Batch Processing. Modeling and Design*; CRC Press: Boca Raton, FL, USA, 2014.
43. Congreso de la República. *Ley 905 (Act 905)*. Congreso de la República de Colombia: Bogotá, 2004; 9 p.
44. DANE. Índice de Precios al Consumidor (IPC) (Consumer price index (CPI)). Available online: <http://www.dane.gov.co/index.php/estadisticas-por-tema/precios-y-costos/indice-de-precios-al-consumidor-ipc> (accessed on 23 January 2020).
45. Banco de la República. Tasa de cambio y captación (Exchange and collection rate). Available online: <https://www.banrep.gov.co/es> (accessed on 20 April 2020).
46. Congreso de la República. *Ley 1943 (Act 1943)*. Congreso de la República de Colombia: Bogotá, 2018; 107 p.
47. Aden, A.; Ruth, M.; Ibsen, K.; Jechura, J.; Neeves, K.; Sheehan, J.; Wallace, B. *Lignocellulosic biomass to ethanol process design and economics utilizing co-current dilute acid prehydrolysis and enzymatic hydrolysis for corn stover*; NREL/TP-510-32438; National Renewable Energy Laboratory: Golden, CO, USA, 2002; 154 p.
48. Alibaba. Products and suppliers. Available online: <https://www.alibaba.com/> (accessed on 28 March 2020).
49. AspenTech. *Aspen Icarus Reference Guide. Icarus Evaluation Engine (IEE) V7.3.1*; Aspen Technology, Inc: Burlington, MA, USA, 2011.
50. Peters, M.; Timmerhaus, K. *Plant Design and Economics for Chemical Engineers*, 5th ed; McGraw-Hill: New York, NY, USA, 2003.
51. Ulrich, G. *A Guide to Chemical Engineering Process Design and Economics*; John Wiley & Sons: Toronto, ON, Canada, 1984.

52. VirtualExpo. Direct industry. Available online: <https://www.directindustry.fr/> (accessed on 28 March 2020).
53. Access Intelligence. Chemical engineering plant cost index. Available online: <https://www.chemengonline.com/> (accessed on May 6 2020).
54. CHEC. Tarifa de energia (Energy fee). Available online: <https://www.chec.com.co/> (accessed on 14 August 2020).
55. Efigas. Tarifa del gas natural (Natural gas fee). Available online: <https://www.efigas.com.co/Nuestros-usuarios/Tarifas> (accessed on 15 August 2020).
56. Aguas de Manizales. Tarifa de agua (Water fee). Available online: <https://www.aguasdemanizales.com.co/> (accessed on 25 August 2020).
57. Aristizábal, V.; Solarte, J.; Cardona, C. Economic and social assessment of biorefineries: The case of coffee cut-stems (CCS) in Colombia. *Bioresour. Technol. Rep.* **2020**, *9*, 100397. <https://doi.org/10.1016/j.biteb.2020.100397>.
58. ChEMBL. Products and suppliers. Available online: <https://www.ebi.ac.uk/chembl/> (accessed on 20 July 2020).
59. Lehto, M.; Sipilä, I.; Alakukku, L.; Kymäläinen, H. Water consumption and wastewaters in fresh-cut vegetable production. *Agric. Food Sci.* **2014**, *23*, 246–256. <https://doi.org/10.23986/afsci.41306>.
60. Guerrero, A.; Ballesteros, I.; Ballesteros, M. Optimal conditions of acid-catalysed steam explosion pretreatment of banana lignocellulosic biomass for fermentable sugar production. *J. Chem. Technol. Biotechnol.* **2017**, *92*, 2351–2359. <https://doi.org/10.1002/jctb.5239>.
61. De Souza, E.; Sellin, N.; Marangoni, C.; Souza, O. The influence of different strategies for the saccharification of the banana plant pseudostem and the detoxification of concentrated broth on bioethanol production. *Appl. Biochem. Biotechnol.* **2017**, *183*, 943–965. <https://doi.org/10.1007/s12010-017-2475-7>.
62. Villarreal, M.; Prata, A.; Felipe, M.; Almeida E Silva, J. Detoxification procedures of eucalyptus hemicellulose hydrolysate for xylitol production by *Candida guilliermondii*. *Enzyme Microb. Technol.* **2006**, *40*, 17–24. <https://doi.org/10.1016/j.enzmictec.2005.10.032>.
63. Nilvebrant, N.; Reimann, A.; Larsson, S.; Jönsson, L. Detoxification of lignocellulose hydrolysates with ion-exchange resins. *Appl. Biochem. Biotechnol.* **2001**, *91*, 35–49. <https://doi.org/10.1385/ABAB:91-93:1-9:35>.
64. Huang, H.; Ramaswamy, S.; Tschirner, U.; Ramarao, B. A review of separation technologies in current and future biorefineries. *Sep. Purif. Technol.* **2008**, *62*, 1–21. <https://doi.org/10.1016/j.seppur.2007.12.011>.
65. Tobajas, M.; Garcia, E. Determination of biomass yield for growth of *Candida utilis* on glucose: Black box and metabolic descriptions. *World J. Microbiol. Biotechnol.* **1999**, *15*, 431–438. <https://doi.org/10.1023/A:1008911630776>.
66. Demain, A.; Phaff, H.; Kurtzman, C. The Industrial and Agricultural Significance of Yeasts. In *The Yeasts. A Taxonomic Study*; Kurtzman, C.; Fell, J., Eds.; Elsevier Science B.V.: Amsterdam, The Netherlands, 1998; pp. 13–19.
67. Øverland, M.; Skrede, A. Yeast derived from lignocellulosic biomass as a sustainable feed resource for use in aquaculture. *J. Sci. Food Agric.* **2017**, *97*, 733–742. <https://doi.org/10.1002/jsfa.8007>.
68. FDA. Microorganisms and Microbial-Derived Ingredients Used in Food (Partial List). Available online: <https://www.fda.gov/food/generally-recognized-safe-gras/microorganisms-microbial-derived-ingredients-used-food-partial-list> (accessed on 10 May 2020).
69. Horn, C.; du Preez, J.; Lategan, P. Protein enrichment of banana plant wastes by yeast cultivation. *Biol. Wastes* **1988**, *24*, 127–136. [https://doi.org/10.1016/0269-7483\(88\)90055-9](https://doi.org/10.1016/0269-7483(88)90055-9).
70. Hopkins, T. Production of Protein with Reduced Nucleic Acid. United States Patent No. 4341802, 27 July 1982.
71. Mizuguchi, T.; Arai, T.; Hirayama, K. Method for Preparing Spray-Dried Microbial Cells. European Patent No. 1281752, 20 October 2010.
72. Goldberg, I. *Biotechnology Monographs*, 1st ed.; Springer: Berlin/Heidelberg, Germany, 1985.
73. Hernández, F.; Morales, Y.; Lambis, H.; Pasqualino, J. Starch extraction potential from plantain peel wastes. *J. Environ. Chem. Eng.* **2017**, *5*, 4980–4985. <https://doi.org/10.1016/j.jece.2017.09.034>.
74. Olsen, H. Enzymatic production of glucose syrups. In *Handbook of Starch Hydrolysis Products and their Derivatives*; Kearsley, M.; Dziedzic, S., Eds.; Springer Science & Business Media: Luxembourg, 1995; pp. 26–63.
75. Pan, Y.; Lee, W. Production of high-purity isomaltoligosaccharides syrup by the enzymatic conversion of transglucosidase and fermentation of yeast cells. *Biotechnol. Bioeng.* **2005**, *89*, 797–804. <https://doi.org/10.1002/bit.20402>.
76. Hernández, J.; Rodríguez, S.; Bello, L. Obtención de jarabe fructosado a partir de almidón de plátano (*Musa paradisiaca* L.). Caracterización parcial (Obtention of fructose syrup from plantain (*Musa paradisiaca* L.) starch. Partial characterization). *Interciencia* **2008**, *33*, 372–376.
77. Rong, M.; Zhang, M.; Liu, Y.; Yang, G.; Zeng, H. The effect of fiber treatment on the mechanical properties of unidirectional sisal-reinforced epoxy composites. *Composites Sci. Technol.* **2001**, *61*, 1437–1447. [https://doi.org/10.1016/S0266-3538\(01\)00046-X](https://doi.org/10.1016/S0266-3538(01)00046-X).
78. Zin, M.; Abdan, K.; Norizan, M.; Mazlan, N. The effects of alkali treatment on the mechanical and chemical properties of banana fibre and adhesion to epoxy resin. *Pertanika J. Sci. Technol.* **2018**, *26*, 161–176.
79. Santa-Maria, M.; Ruiz-Colorado, A.A.; Cruz, G.; Jeoh, T. Assessing the feasibility of biofuel production from lignocellulosic banana waste in rural agricultural communities in Peru and Colombia. *BioEnergy Res.* **2013**, *6*, 1000–1011. <https://doi.org/10.1007/s12155-013-9333-4>.
80. Zahan, Z.; Othman, M. Effect of pre-treatment on sequential anaerobic co-digestion of chicken litter with agricultural and food wastes under semi-solid conditions and comparison with wet anaerobic digestion. *Bioresour. Technol.* **2019**, *281*, 286–295. <https://doi.org/10.1016/j.biortech.2019.01.129>.

81. Bachmann, N. Design and engineering of biogas plants. In *The Biogas Handbook. Science, Production and Application*; Wellinger, A., Murphy, J., Baxter, D., Eds.; Woodhead Publishing Limited: Cambridge, UK, 2013; pp. 191–227.
82. Moran, A. *An Applied Guide to Process and Plant Design*; Elsevier: Amsterdam, The Netherlands, 2015.
83. Sirola, J. Industrial applications of chemical process synthesis. In *Advances in Chemical Engineering*; Anderson, J., Ed.; Academic Press: Cambridge, MA, USA, 1996; Volume 23, pp. 1–62.
84. Demir, I. Fixed offshore platform design. In *Handbook of Offshore Engineering*; Chakrabarti, S., Ed.; Elsevier: London, UK, 2005; pp. 279–417.
85. Douglas, J. *Conceptual Design of Chemical Processes*; McGraw-Hill: New York, NY, USA, 1988.
86. Benedek, A. Anaerobic Fermentation to Produce Biogas. United States Patent No. 10144664, 4 December 2018.
87. Hamer, G. Recycle in fermentation processes. *Biotechnol. Bioeng.* **1982**, *24*, 511–531.
88. Hagen, M.; Polman, E.; Jensen, J.; Myken, A.; Joensson, O.; Dahl, A. *Adding Gas from Biomass to the Gas Grid*; Report SGC 118; Swedish Gas Center: Malmö, Sweden, 2001; p. 142.
89. Allegue, L.B.; Hinge, J. *Biogas Upgrading. Evaluation of Methods for H₂S Removal*; Danish Technological Institute: Taastrup, Denmark, 2014; p. 31.
90. Souza, E.; Liebl, G.; Marangoni, C.; Sellina, N.; Montagnoli, M.; Souza, O. Bioethanol from fresh and dried banana plant pseudostem *Chem. Eng. Trans.* **2014**, *38*, 271–276. <https://doi.org/10.3303/CET1438046>
91. Franzén, C.; Lidén, G.; Niklasson, C. A new method for studying microaerobic fermentations. II. An experimental investigation of xylose fermentation. *Biotechnol. Bioeng.* **1994**, *44*, 429–435. <https://doi.org/10.1002/bit.260440405>.
92. CSIMarket. Miscellaneous Fabricated Products Profitability. Available online: https://csimarket.com/Industry/industry_Profitability_Ratios.php?ind=109 (accessed on 3 October 2022).
93. IEA Bioenergy. Biorefineries: Adding Value to the Sustainable Utilisation of Biomass. Available online: <http://www.ieabioenergy.com/wp-content/uploads/2013/10/Task-42-Booklet.pdf>. (accessed on 10 July 2019).